Materials-Affected Manufacturing in Precision Machining

A Thesis
Presented to
The Academic Faculty

by

Omar Fergani

In Partial Fulfillment
of the Requirements for the Degree
Master in the
School of Georges Woodruff School of Mechanical Engineering

Georgia Institute of Technology
December 2014

MATERIALS-AFFECTED MANUFACTURING IN PRECISION MACHINING

Approved by:

Dr. Steven Y Liang, Advisor
School of Mechanical Engineering
Georgia Institute of Technology

Dr. Shreyes Melkote
School of Mechanical Engineering
Georgia Institute of Technology

Dr. Christopher Saldana
School of Mechanical Engineering
Georgia Institute of Technology

Dr. Yang Jianguo, co-Advisor
School of Mechanical Engineering
Donghua University, Shanghai, PRC

Date Approved: [Nov-10-2014]

DEDICATION

To my parents:

Fatima Gadi

Addi Fergani

ACKNOWLEDGEMENTS

I would like to express my gratitude to my supervisor, Dr. Steven Liang, whose expertise, understanding, and patience, added considerably to my graduate experience. I would like to thank the other members of my committee, Dr. Shreyes Melkote, Dr.Christopher Saldana, and Dr. Jianguo Yang for the assistance they provided at all levels of the research project and for reviewing my thesis. Special thanks goes out to Dr. Ismail Lazoglu, without whose motivation and encouragement I would not have considered a graduate career in mechanical and materials research.

I must also acknowledge my colleagues from the PMRC at Georgia Tech: Alexander Shih, Manik Rojora, Noris Gallandat and especially Yamin Shao with whom I enjoyed spending many hours brainstorming. I would like to thank Steven Sheffield and Louis Boulanger from the machine shop for their valuable help, as well as Glenda Johnson for her help and advice.

I would also like to thank my parents, my brother and sister for the endless support they provided me through my entire life and in particular, I must acknowledge my fiancée Viktoria and my friends Youssef and Souhayl, without whose love, encouragement and editing assistance, I would not have finished this thesis. I would like to acknowledge the Boeing Company for funding this project.

TABLE OF CONTENTS

LIST OF TABLES

LIST OF FIGURES

SUMMARY

The influence of different microstructural attributes on the material properties such strength, hardness, residual stress or other physical properties are very well understood. During the manufacturing of mechanical parts utilized in important industries such as energy, aerospace or biomedical, the effect of the processing in term of thermal and mechanical loading is very important as it is directly influencing the microstructure evolution and the properties. The understanding of how the manufacturing process such as high precision machining will affect first the microstructure and therefore the part properties. In this work, we propose the Materials-Affected Manufacturing (MAM). It is a new paradigm helping to understand the interaction between the manufacturing process parameters, materials microstructure attributes and the properties. This is solved using a computational approach using an iterative blending to relate different models. Residual stresses are also studied. An enhanced analytical model is proposed. The model is capable for the first time to predict analytically the residual stress regeneration in the multi-step machining problem. An enhancement of the existing model is proposed. The (MAM) method was applied to the case of turning process of Aluminum 7075. The average grain size and the crystallographic texture were predicted and validated experimentally. The residual stress regeneration was computed for the case of milling of Aluminum 2024. Experimental validations using X-ray technique were performed for validations.

CHAPTER I

INTRODUCTION

The recent advances in precision machining technology contributed significantly to the enhancement of human life through the development of higher quality and more complex components used in daily life technology. These achievements are possible because of the results of research programs on machines tools, materials and control theory. The definition of precision machining in the 21st century went beyond the traditional geometrical understanding of precision. High accuracy in metrology is possible thanks to high resolution controller. In the manufacturing community, the term precision machining refers more and more to the capacity to manufacture complex part based on very hard to cut materials while being able to control the evolution of the part properties. The materials properties of a workpiece are known to have a great impact on it functionality. Mechanical properties, physical properties as well as some microstructure attributes are now part of the requirement requested during the precision machining of a component. Due to the recent advances in technology, manufactured parts are more and more working under very hard conditions. Applications in aerospace such as turbofans or energy production such as turbine are very critical and request a high tolerance as well as resistance to high temperature and pressure conditions.

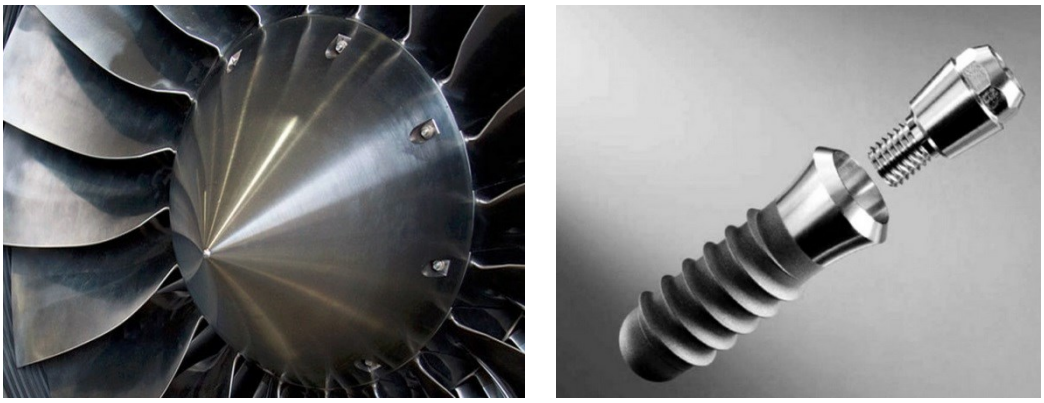

Figure 1: Turbofan propeller and dental implant made of Titanium alloy.

Other uses in biomedical application request light-weight materials with high resistance to cyclic loading. Materials scientists were traditionally were at the front of the problem resolution; they develop and produce continuously new materials that are temperature resistant such as Nickel based alloy and Titanium alloy as shown in Figure 1). More recently, and typically for biomedical application, the emergence of new processes such as SPD (Severe Plastic Deformation) based like ECAP are capable of producing materials with very high strength due to the grain refinement happening, Figure 2).

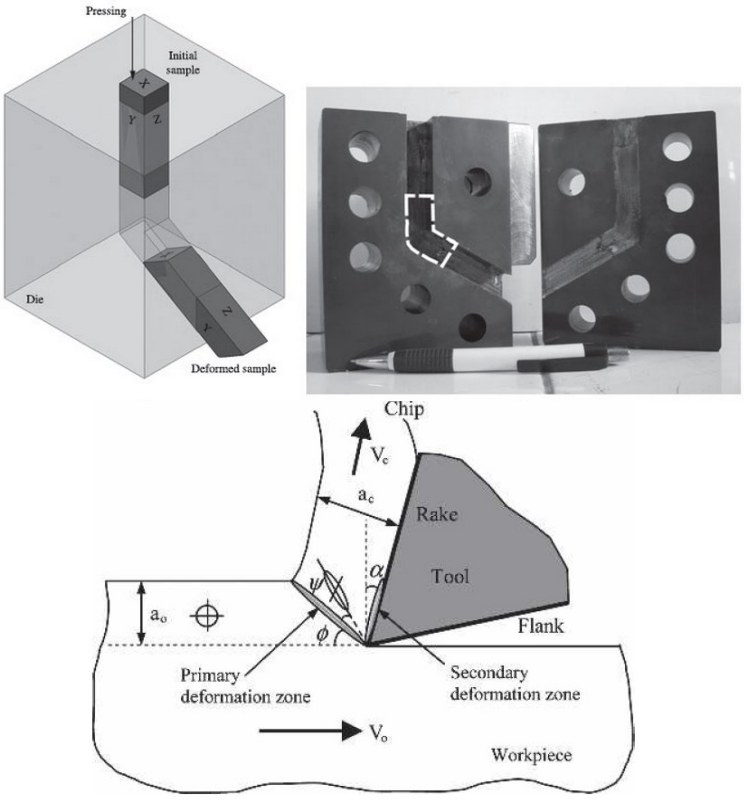

Figure 2: ECAP processing method.

As the manufacturing and especially the machining process are the final step before the product utilization, it is important to understand how the cutting process will affect the product final quality and if the machining process as an SPD process can enhance the properties of the machined surface. For many years, people were interested in the surface finish quality or roughness. Recently, new surface integrity parameters are to be investigated before the utilization of such components. Manufacturing and quality engineer are now interested in the residual stress. The machining induced residual stresses are actually critical on the crack propagations, resistance to corrosion as well as fatigue behavior. Finally, more requirement coming from leader industries such as the nuclear one, introduced new requirement on the grain size and other properties such as the hardness. It is obvious that the machining

process will affect the properties of the workpiece. The large thermo-mechanical loading introduced due to high speed application of dry machining configurations will undeniably influence the stability of microstructure ad therefore influence the materials properties. It is important to understand the thermo-mechanical loading induced by machining. It appears that machining induces the larges deformations with a very high rate. The machining is also a source of heating, temperature during the machining of some hard to cut materials can be as high as 1300° degrees. Based on all this, it is clear that relating the process mechanics or more accurately the process input to the properties of the workpiece as well as the microstructure is critical in order to optimize the machining process. A design tool capable of helping the manufacturing engineer choosing the right machining conditions is therefore necessary to achieve desirable properties.

Figure 3) shows the context of this research, such a tool set will be capable of relating the manufacturing science knowledge that includes cutting forces and temperature predictions to a more general continuum mechanics approach solving the strain, strain rate and stress experienced by the workpiece materials. Based on this, tools developed by materials scientist can be implemented in order this time to understand how the microstructure and therefore properties will evolve. We can imagine such a tool providing valuable information to the design engineer. This approach will reduce the product life cycle as well as provide a platform to optimize the manufacturing process.

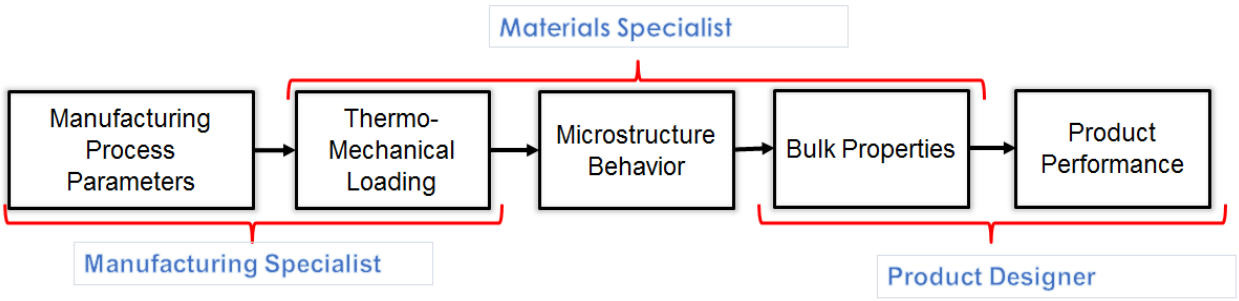

Figure 3: Material manufacturing and design interactions.

In the context of this identified need. Some research questions are imposed naturally and need to be addressed in order to solve this research challenge. Is the machining process capable of affecting the workpiece properties and microstructure? Through which mechanisms the machining process will affect the microstructure? How to relate the process input parameter to the properties of the workpiece? Is the evolution of properties will affect the process mechanics?

To addressee this question, a step by step analysis is applied and a research strategy is proposed in order to solve the research questions.

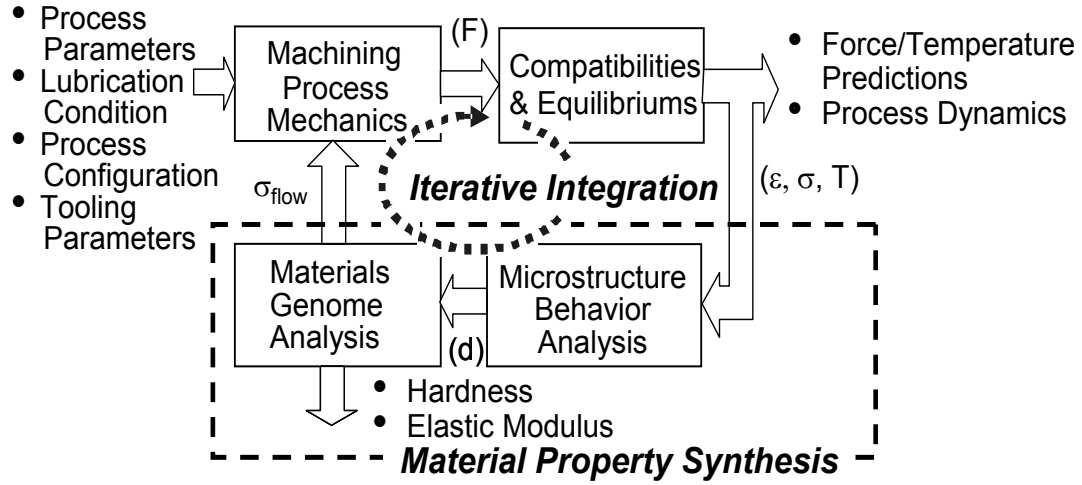

Figure 4: Materials-Affected Manufacturing paradigm.

The Materials-Affected Manufacturing (MAM) approach consists of relating the input of process parameters to the materials properties through a defined path. Figure 4) shows the MAM paradigm. After predicting process forces and temperature, the equilibrium and compatibilities are solved in order to derive the generated stresses, strain and strain rate. Then, the materials synthesis is used. In the materials synthesis, we have two analysis steps, the microstructure evolutions predictions. In this step and based on the thermo-mechanical load, the evolution of some microstructure attributes that have a direct influence on the materials properties is predicted. Grain size, texture, etc. are predicted and used in the next step. The last step of the materials synthesis is the materials genome analysis. In this step, the mechanical, physical properties such as hardness, flow stress and moduli are predicted based on microstructure attributes. Finally, it is important to notice that the process prediction will iteratively be affected by the evolution of the properties. The cutting forces are expected to increase if the flow stress increases, the opposite is also true.

The implementation of MAM as a powerful predictive tool set will allow a drastic enhancement of the manufacturing process optimization and control. A physics driven understanding of the part final properties and therefore some quality aspect will lead to an enhancement of the standards.

Residual stress is an important part of the global image that needs to be investigated. During the machining process, one of the most important attributes affecting the functionality is residual stress remaining in the workpiece. It is obvious that the understanding of residual stress is critical. The nature of residual stress (tensile vs compressive) will play a key role in the crack propagation. The peak compressive in subsurface will provide helpful information about the fatigue behavior. The global distribution in all directions is also important for dimensional accuracy issues such as

distortions. Different research investigated residual stresses in machining. The accuracy of the output was always complicated to evaluate especially that most of the proposed predictive models are based on numerical solution such as FEM. The large computational time as well as the limited physics based understanding was always at the origin of the poor usage of this method. Recent research in the field of analytical modeling proposed powerful method to predict residual stress using better model and especially a short computational time. However, theses mathematical models considered a simple case of one machining pass as well as other simplifying assumptions that affected strongly the surface residual stresses.

In this work, and for the first time, an enhanced mathematical model for residual stress is proposed. Large number of assumptions were reduced or corrected in order to enhance the predictive capacities. The model was also adapted for the uses of multi-steps machining process. An algorithm was proposed for this purpose. The nonlinear cyclic plasticity was also included in order to enhance the predictions. Experimental work is performed on aluminum alloy for the milling process. It is important to understand the state of art in the research of materials, manufacturing and mechanics. How these challenges are handled and what are the models that we can explore in order to achieve the research objective. The next chapter covers the existing research and results regarding the process mechanics, microstructure evolution in machining and finally the properties.

CHAPTER II

LITERATURE REVIEW

2.1 MICROSTRUCTURE EVOLUTION IN MACHINING

2.1.1 Grain evolution

During machining a high amount of shear stress, strain and strain rate are experience by the materials. It is also known that during the cutting process, most of the plastics deformation energy is transformed into heat. Therefore, the machining process will induce a very high temperature especially in some specific machining configurations such as dry cutting. Also to mention is the non-uniform temperature gradient, generated by machining, which affects the materials microstructure and the surface integrity [1] [2] [3]. Those mixed mechanical and thermal loadings, applied by the cutting tool on the workpiece, are expected to drive and activate different phenomena within the materials that will strongly affect the microstructural attributes such as the grain size, texture and dislocation density.

One of the main microstructural attributes that directly affects the materials properties is the average grain size. The grain size can affect the physical properties such as the conductivity as well as mechanical properties like the flow stress or the hardness. Different studies investigated the effect of machining on the average grain size on the surface [4] [5]. The grain size variation was mainly attributed to the dislocation dynamics and the dynamic recrystallization happening due to the large strain and strain rate induced by the machining process as reported recently by [6] . Although the mechanical aspect of the machining process (i.e. strain and strain rate) might be the dominant driving force of microstructural changes on the workpiece surface, the

temperature, conducted through the whole workpiece, will inevitably affect the microstructure in the subsurface region depending on the materials system as shown in Figure (2). Therefore in some thermo-mechanical processing, grain growth is observed and attributed to different sources. Recent studies highlighted this fact through the investigation of diffusion based grain growth, generally considered as a thermally activated phenomenon [7]. This was reported in [8] where a grain growth was observed during the machining of aluminum alloys in the subsurface area. Therefore the grain refinement and grain growth are expected to happen during the machining process at different locations in depth and can even be a competing behavior. In a previous study [8] , the microstructure evolution in the orthogonal cutting was investigated. In [9] the effect of strain and strain rate were investigated in an orthogonal cutting situation with different cutting speed conditions. It was observed that for OFHC Cu the high strain is generating a very refined structure of grain, while at high strain rates, the effect of temperature is limiting the refinement process. This can be attributed to a possible grain growth that was not investigated in the case of machining. In a different work [10] it was similarly investigated that this microstructure evolution in the orthogonal machining of pure Copper and pure Titanium, a framework describing the evolution of the microstructure as a function of strain, strain rate and temperature, was given. It was observed that at high and low strain rates and relatively high temperature an equiaxed nano-sized grain were obtained. While at high strain rate and high temperature either a mixed structure with micron and nano-sized grains or twinned nano-structure were observed. This suggested that the combined thermo-mechanical load will generate a competing behavior that can be understood and modeled, based on physical modeling.

2.1.2 Texture

The texture or crystallographic orientation in metals and alloys is one of the main microstructural attributes that affects their mechanical properties and therefore the materials behavior. The crystallographic anisotropy also has a significant effect on the manufacturing process, especially metal cutting at micro-scale in which the grain level characteristics are important. For decades, investigations of the crystallographic anisotropy were conducted to understand the process product interactions. In fact, extensive experimental work using recent available technologies such as X-ray diffraction and EBSD has opened the opportunity for a better understanding of the crystallographic anisotropy, especially in the machining processes. Pioneering work that investigated how the machining process affects the surface texture was conducted in an ultra-precision context of β-Brass using a diamond tool by [11]. They discovered that the cutting forces changed regarding the crystallographic orientation. Using FEM, a strain gradient based approach was used by [12] to investigate the micro-machining of single crystal FCC material. Recent work by [13] experimentally investigated the relationship between the specific cutting energy and the crystal orientation of pure aluminum. They discovered that the specific energy relied more on the crystal orientation rather than the process parameters and this specific energy can vary between (25 MPa up to 450 MPa). The same authors proposed in [14] a rate sensitive plasticity model to predict accurately the cutting forces in the micromachining of FCC single crystal materials. This model considered the hardening of the materials as well as the effect of lattice rotation. Hence, a strong relationship between the crystallographic orientation on which the cut is made and the wear rate of a cutting tool can be established as suggested by the recent studies of [15] based on a diamond cutting tool. Further, [16] has proven that the crystallographic orientation

affects the surface roughness, since the amount of machine tool vibration depends on the cutting direction, these experiments were made on single crystal copper using a diamond tool. The severe plastic deformation generated by the machining process was investigated by [17], in their study, the microstructure evolution was analyzed in the PDZ (Primary Deformation Zone) and the SDZ (Secondary Deformation Zone). Researchers have discovered a microstructure evolution during the machining process using SEM image and EBSD investigations. The crystallographic anisotropy is also important to investigate, different theoretical analysis were made to capture the mechanisms describing the relationship between the manufacturing process mechanics and the texture evolution. In the machining field, there exist models that were proposed to investigate this issue. A micro-plasticity model was proposed by [18] where the shear angle variation was investigated as a function of the main crystal orientation to understand how the cutting force were affected in the case of micromachining. They concluded that the most likely shear place is the one that has the most negative texture softening factor among the ones with the minimum shear strength. In the same way [19] implemented the crystallographic orientation in the flow stress and proposed an analytical method to predict the cutting forces in the micromachining of brittle materials. This approach enabled the possibility to accurately predict the ductile brittle transition point. In a very recent evolution of the modeling work, [20] and [21] presented a flow stress model capturing the flow stress evolution as a function of microstructural attributes such as the dislocation density and the average grain size. Important experimental investigations performed by [22] shown that during the cutting of single crystal aluminum of known orientation under the same cutting conditions, the cutting forces and the chip thickness ratios vary with the crystal orientation. All these recent evolution in the experimental and modeling

work contributed to enhance the understanding of the interaction between microstructural attributes and the metal cutting process. However, few studies have been done in term of physics-based model to capture the texture evolution during and after machining. Predicting the anisotropy is therefore an important issue that needs to be addressed in order to build an accurate understanding of the machining processes. During the machining process, a large plastic deformation is taking place. Mechanical and thermal loading are induced while driving microstructural changes on the workpiece surface and subsurface. Fundamental work has been conducted to understand accurately the state of stresses and strain during the machining process [23]. To the best of the author's knowledge, no physics-based model was proposed in the machining community to fully address and capture the texture evolution in the cutting processes.

Previous works by [24] presented an accurate model to predict temperature. Theoretical models based on the physics of large plastic deformation were introduced by [25] to capture the crystallographic anisotropy evolution for large deformation of polycrystals. This theory was derived from a single crystal constitutive relation by solving integral equations from the field equations. A self-consistent approach is developed, where each grain is assumed to be a single ellipsoidal inclusion in a homogeneous equivalent medium as introduced previously by [26]. This approach has been used extensively in predicting the texture for basic testing processes such are compression and tension. Researchers at Los Alamos National Laboratory developed a Viscoplastic (VP) self-consistent (SC) robust and validated code to predict the texture called VPSC. This code was used by [27] to predict the texture evolution of zirconium. Other theories where introduced to predict texture for polycrystals. The

statistical continuum theory was used by [28] and offered an alternative to the self-consistent approach. The statistical method has been proven for tension, compression

2.2 RESIDUAL STRESS

During the last few years the understanding of the effect of machining parameters on the residual stress profile contributed to the enhancement of surface integrity in machining. As a consequence enhancement of part functionality needed in aerospace, energy and medical applications become possible as reported in [29] . Analytical model have shown their capacity to predict residual stress accurately in a very short computational time. They also offer the possibility to investigate the physics of the phenomena in contrast to FEA methods, known for their very large computational time and their small physics based interaction. In [30] and [31]. Based upon this knowledge, a new analytical model to predict residual stress induced distortion was proposed [32]. Unfortunately, these models were based on a simplifying assumption that reduces the complexity of machining (Turning, milling) to a single pass operation. As a consequence, the residual stress regeneration after each pass was not considered. Different behavior induced by the multi-steps nature of the machining processes such as cyclic plasticity hardening or the evolution of initial condition as well as the residual strain history evolution were not considered. The model proposed in this research will enable to integration of the analytical prediction based tool into the design and manufacturing life cycle of a part as shown in Figure (1). As a result, a faster residual stress prediction can be performed based on the output of the CAM proposed G-Code.

Previous researchers were interested in the problem of residual stress regeneration. FEA was used to investigate the effect of different machining passes on the final

residual stress profile. In [33] recently investigated the effect of multi-step orthogonal cutting using a constant cutting conditions. It was discovered that due to the increase of temperature during the last step, a tensile surface residual stress was predicted. The authors of this study highlighted the fact that large amount of simplification were made in order to reduce the large computational time. In another study [34], it was discovered that controlling the undeformed chip thickness can help in order to optimize the surface residual stress from tensile generally generated during roughing to compressive while using a small undeformed chip thickness during the finishing step. Another conclusion was that the specific cutting energy for similar steps changed due to the change in the materials flow characteristics and therefore the shear angle. Due to the large computational time, machining validation was performed for very small cutting speed (13 mm/min) to avoid temperature rise. The few previous research effort that focused on the residual stress prediction in multi-step helped to understand the fundamentals mathematical challenges as well as showing different limitations due to simplifying assumptions as well as the limitations associated to the FEA method.

CHAPTER III

EFFECT OF MACHINING PROCESS ON AVERAGE GRAIN SIZE

3.1 INTRODUCTION

The microstructure plays a key role in determining the properties of a material. Grain size, is particularly important as it is related to the processing history of the material. Grain size and shape are important to investigate in order to understand the materials behavior as well as predicting the properties. Empirical models introduced by Hall-Petch to relate strength to the grain size or Nabarro-Herring to capture the creep effect are the some of the example that illustrates the key role of the grain size as shown in Figure 5).

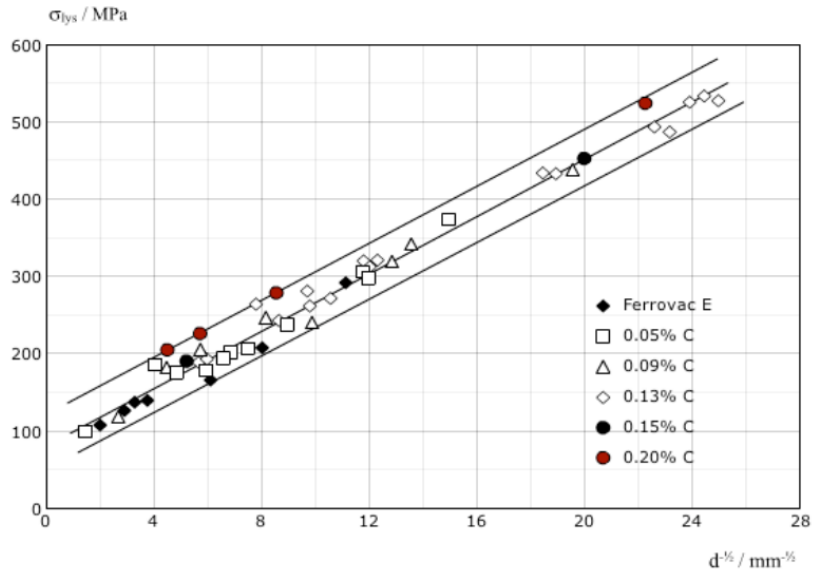

Figure 5: The relation between materials strength and the grain size (Hall-Petch effect [35]).

As a direct consequence of the Hall-Petch empirical equation, different research groups started studying the effect of machining on the average grain size. New

methods based on orthogonal cutting was developed in order to achieve a refined grain structure based on the ECAP method. Machining, especially the shear zone called the primary deformation zone was investigated. Nano-indentation results as well as SEM scanning showed some strong gradient happening due to the shearing. In the shearing zone where strain can be very high microstructure changes was observed. Using TEM, the effect of the severe plastic deformation was captured. Grain refinement was captured as shown in the Figure 6).

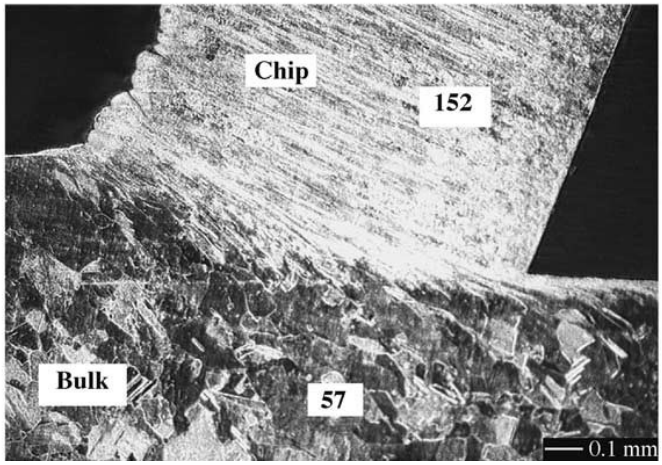

Figure 6: Metallography of the shear zone area [36].

Due to the instability of microstructure, the refinement stability was also investigated for different materials at different heat treatment condition [35]. However, most of these initial studies focused on the chip. Only few studies investigated the machined surface microstructure evolution and especially the grain size. In a recent study, the fundamental understanding of the effect of machining parameters on the grain evolution was investigated in the case of single crystal copper [36]. The main parameter affecting the refinement is related to the rake angle as the rake angle will define the amount of strain induced on the workpiece. They also discovered the same level of deformation on the chip and the machined surface to 10 μm beneath the surface. The effect of depth of cut was very minor. All this study was however

performed in the case of single crystal material and at very low cutting speed (1mm/s to 10mm/s). It is known that during the regular machining process, the cutting speeds are higher and can go to more than 800 m/min in the case of turning process. Further most of the materials used in industry are alloys. Therefore the effect of precipitates may affect the microstructure behavior. In this chapter, the different mechanisms that can affect grain growth in machining all considered. The effect of machining temperature is also included. The model is developed and validated for the case of AA-7075. Experimental grain size measurements are performed at each point in the depth of the workpiece. Predictions are performed and validated. Finally, this model is used to capture the effect of the evolution of machining parameters on the average grain size. Preliminary experiments and measurements showed that in the conventional machining, grain can experience growth and refinement. Refinement is mainly due to dynamic recrystallization (DRX), while grain growth source is yet to be determined accurately. Most of studies showed that due to the high heating rate during the machining growth can be experience due to grain boundary diffusion due to the relaxation of dislocation in order to achieve a low energy level for more stability. Figure 7) show an EBSD image of before and after machining. We can clearly observe refinement and growth of some grains. Details of the modeling and more physics argument are explain in the next section.

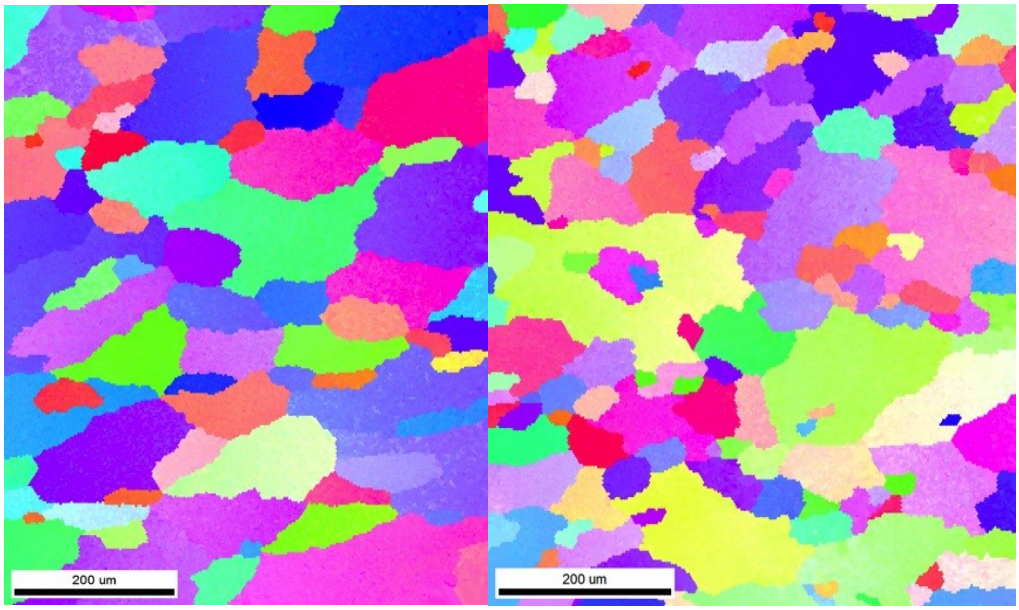

Figure 7: EBSD scan of the machined surface before and after machining.

3.2 MODELING

Based on the analysis of machining experiments, a surface average grain prediction model, considering the different thermo-mechanical loading experience, generated by the machining process in the profile of the workpiece is developed. Based on the nature of the multi-step machining process, it is assumed that two main behaviors are observed, a severe refinement driven by the large plastic deformation that activates the dynamic recrystallization and the grain growth driven by the temperature. It is also assumed that these two competing behaviors are happening at the same time. Therefore a linear superposition of these two behaviors is applied using the method of average. The refinement function (d^{-}) on the surface was predicted using the Arrhenius equation from where the well-known Zener-Hollomon parameter is derived. It uncovers the approximate hyperbolic law between the Z parameter and the flow stress using Johnson-Cook. $\mathrm{Z} = \dot{\varepsilon}\ \exp(\mathrm{Q}/\mathrm{RT})$ where $\dot{\varepsilon}$ the strain-rate predicted using the process mechanics approach presented in the previous section, $R = 8.3145 J/(K\,mol)$, R is the universal gas constant; $Q = 116.7\,kj/mol$, is the

apparent activation energy for mechanical deformation process; T is the machining temperature K. The Zener-Hollomon parameter Z can be written in term of the machining flow stress σ. The activation energy was chosen from the literature. As the DRX activation energy depends on the temperature and the strain rate, this constant was selected in a range of temperature and strain rate close to the once experienced in the machining process. Details about the activation energy can be found in [37].

$$Z = A(\sinh \alpha\sigma)^n \quad (1)$$

σ is the flow stress induced by the machining operation and calculated using Johnson-Cook as described [38]. The average grain size variation during the machining operation was captured using an incremental approach introduced previously by [39]. The grain growth phenomenon is known to be induced by temperature when it achieves the activation level. Grain growth takes place by grain boundaries diffusion processes when the process time and temperature are large enough and the heating rate are fast. This therefore can happen during long machining operations inducing high temperature and strain rate as presented in [40]. Thermally activated cross-slip is the mechanism commonly believed to be responsible for growth based on thermal activation of vacancies without long rang diffusion that will control dynamic recovery rates during plastic deformation as presented by [41]. During the machining of AA-7075, temperature was measure using thermocouple and simulations were performed. The machining temperature was always equal to 0.5 T_m or greater. The grain growth during the machining d^+ is used in this study based on the models presented by [42] and [43] and shown in Eq. (5). During the cutting operation the heating rate is assumed to be constant during the heating as shown in Figure.3, therefore the equation yielded to a new equation where the final grain size is function of the heating rate $\dot{T}$. The initial temperature T_i, final temperature T_f and n, k. Therefore, equation

(2) presents a unified model based on the consideration of grain growth under the temperature effect and the grain refinement introduced by the machining severe plastic deformation.

$$\begin{cases} d^{-} = d_0 . b . Z^m, \\ d^{+} = \left(\frac{KR}{\dot{T}Q}\right)\left({T_f}^2 \exp\left(\frac{-Q}{RT_f}\right) - {T_i}^2 \exp\left(\frac{-Q}{RT_i}\right)\right) + d_0^n, \end{cases} \quad (2)$$

The final surface grain size is therefore calculated assuming both component of Eq (2) using the average concept. $d = \frac{d^{+}+d^{-}}{2}$.

3.3 EXPERIMENTAL VALIDATIONS

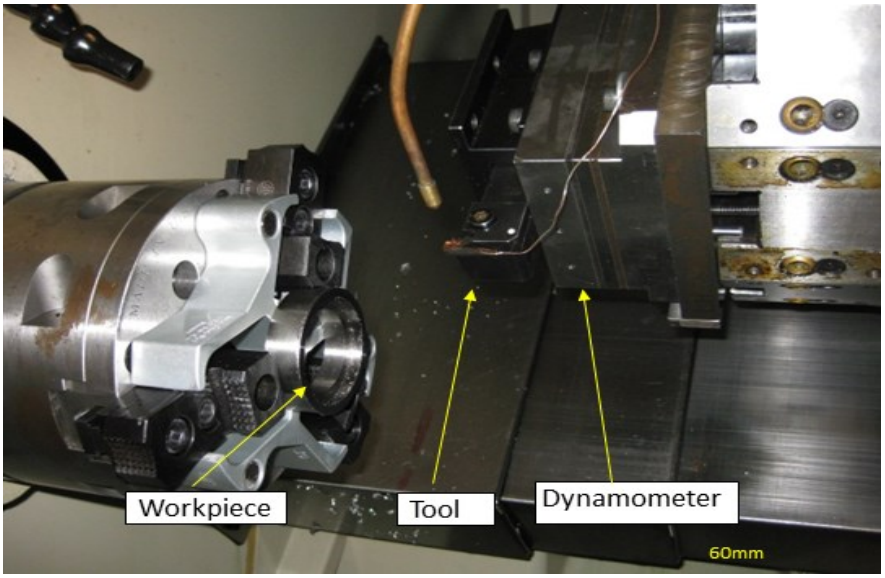

Figure 8: Machining configuration and experimental setup.

Machining experiments were conducted for turning of Aluminum alloy AA-7075-T6, heat treated. The initial material characterization revealed an initial grain size of 35µm, while the initial Hardness was 154 kg/mm^2. A dry machining was conducted using a PCBN cutting insert with a rake angle of 8 degrees (Figure (7)). The cutting insert was fresh as at each new experiment a new insert was used. Depth of cut was changed from 0.5mm, 1mm and 2mm. feed was of 0.1mm/rev and cutting speed was

0.5m/s. In this first set of experiments on AA-7075-T6, the result of the process mechanics suggesting the existing of two affected area in the workpiece. Average grain size was measured before and after the machining process. In this first experiment, the cutting conditions were selected in order to make sure a high cutting forces temperature will be generated, as we can verify the case where growth and refinement has to be superposed. For the second material AA-6061-T6 [44], an orthogonal machining configuration with a 5° rake angle and 100 µm depth of cut and a very low cutting velocity of 10mm/s was applied in order to avoid temperature rise during the machining. The bulk materials average grain size was found 75 µm while the hardness was 110 kg/mm^2. The microstructure evolution across the shear plane from the bulk to the chip was investigated using a sequence of TEM taken before and after machining as shown in Figure (11).

For AA-7075-T6, $\alpha \; and \; n$ are two constants found as $0.012\, mm2/N$ and 5.3 respectively [45]. A is given as $20 * 10^9\, s^{-1}$. $n = 3.2\,, K = 28.5\, 10^{-4}$ and $Q = 116\, kj/mol$ are the grain growth exponent, the rate constant and the activation energy. The temperature was predicted based on the approach presented by [46]. Each of these constants is assumed to be independent from temperature $R = 8.3145 J/(K\, mol)$ is the gas constant. The two sets of experiments were selected in order to validate the average grain size prediction model. In the second set of experiments, we assume that the effect of temperature can be neglected therefore we expect only refinement. However, for the case of AA-7075 both grain growth and refinement are expected.

The grain refinement model for AA-7075 was implemented and calculated. Figure 9 shows how the Zener-Hollomon parameter will drive the refinement of the grains. The predicted final grain is around 3µm. The grain growth was calculated as a

function of the cutting temperature. Using the iterative approach and the superposition method, the final grain size after machining was found to be around 25 μm.

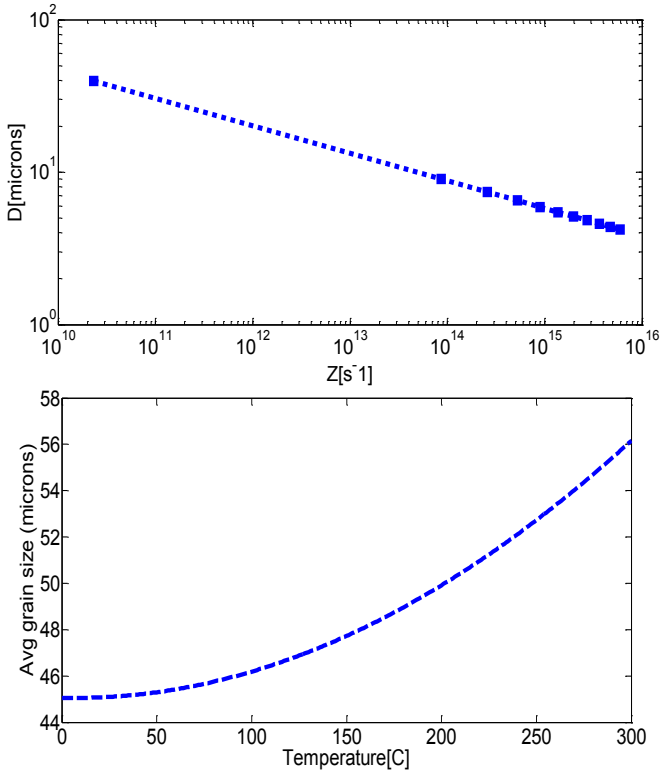

Figure 9: Zener-Hollomon parameter for grain refinement and growth for AA-7075 alloy.

However, for the case of AA-6061 alloys, the temperature was not included in the model and the grain refinement was predicted to be reduced to values as small as few nanometers as shown in Figure 10). In fact, based on the experimental results captured using TEM microscope, it is clear that on the machined surface the average grain was less than a micron. Hence, the refinement induced by dynamic recrystallization and captured in this model using the Zener-Hollomon parameters proves a high capability to capture the trend of refinement during non-thermal processing.

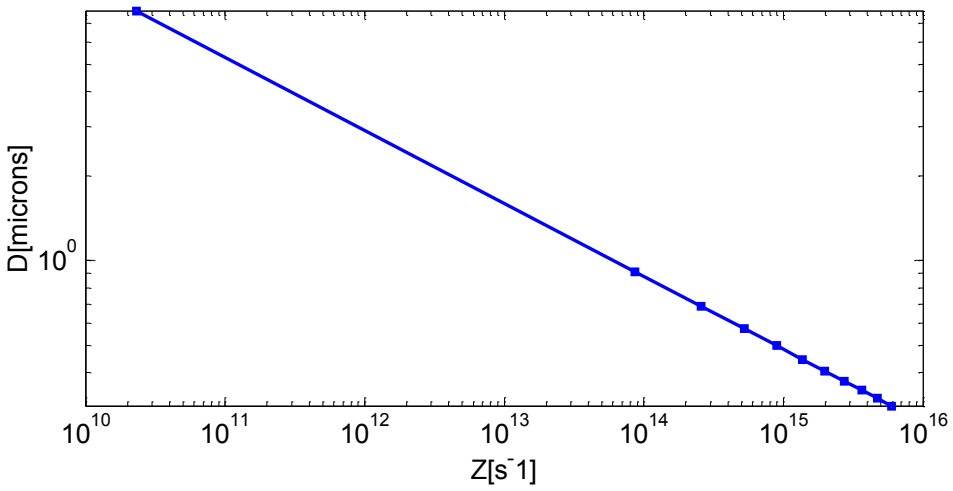

Figure 10: Zener-Hollomon parameter and grain refinement in the machining of AA-6061 alloy.

In this study, an iterative computational approach was used in order to predict and blend the evolution of grain growth and refinement. This computational approach can be shown in Figure 11), where the average grain size at the steady state of the machining was calculated at the convergence point in this case around (300000 iterations). This shows that the iterative approach used as a computational technique to predict the effect of machining was converging to the correct value. Further the computational time was very short compared to numerical methods. The total computational time was in order of few minutes.

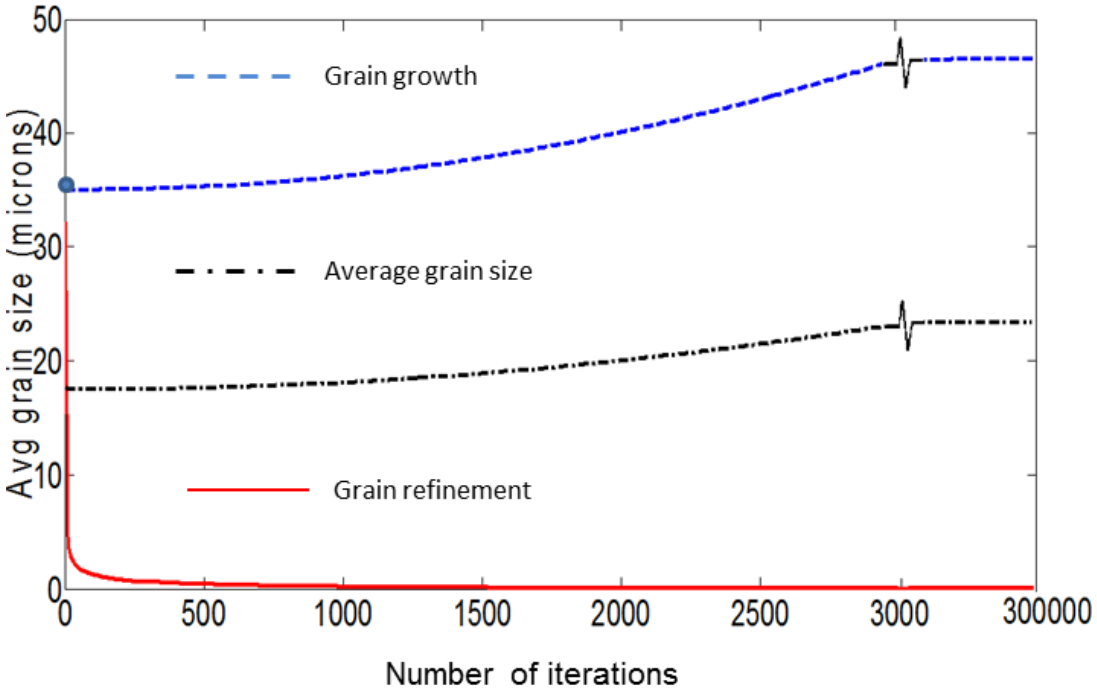

Figure 11: Iterative convergence of the grain size.

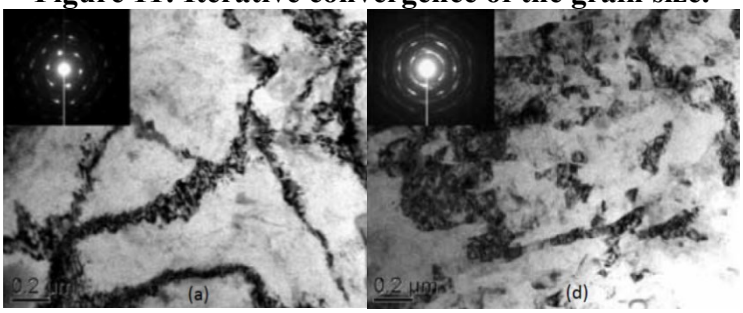

(a)

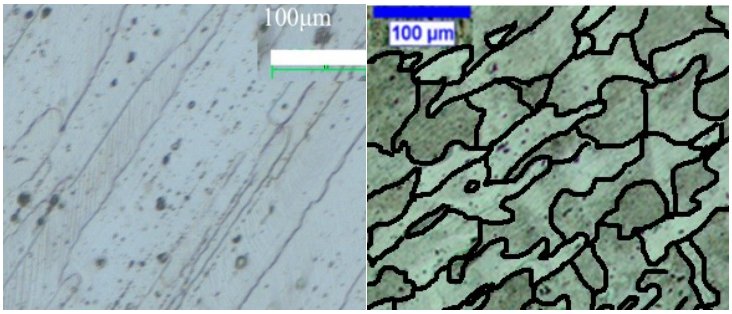

(b)

Figure 12: (a) Average grain size before and after machining of AA6061-T6 [45] (b)AA7075-T6 before and after machining.

On the machined surface, the new grains showed a new structure. The equiaxed initial structure changed to smaller elongated grains. Very small grains that are a result of

dynamic recrystallization were also observed and contributed to the reduction of the average grain size as shown in Figure 12). Knowing that the machining process will induce high shear stress and strain, it is therefore expected to observe a texture evolution on the machined surface as suggested by previous study [47]. In order to verify the proposed model experimental investigation of average grain size as a function of depth is proposed in Figure 13). It shows a superposition of the measured grain at different depth and the predicted values. This shows that the model is capable of predicting the grain size at different locations depending on the thermo-mechanical history of the location.

Average grain size was measure on a two dimensional sections of the microstructure. The method is based on the ASTM by measuring the number of grain per inch^2. If N is the count average number of grains per inch2, ASTM grain size number n is give as fellow: $N = 2^{(n-1)}$.

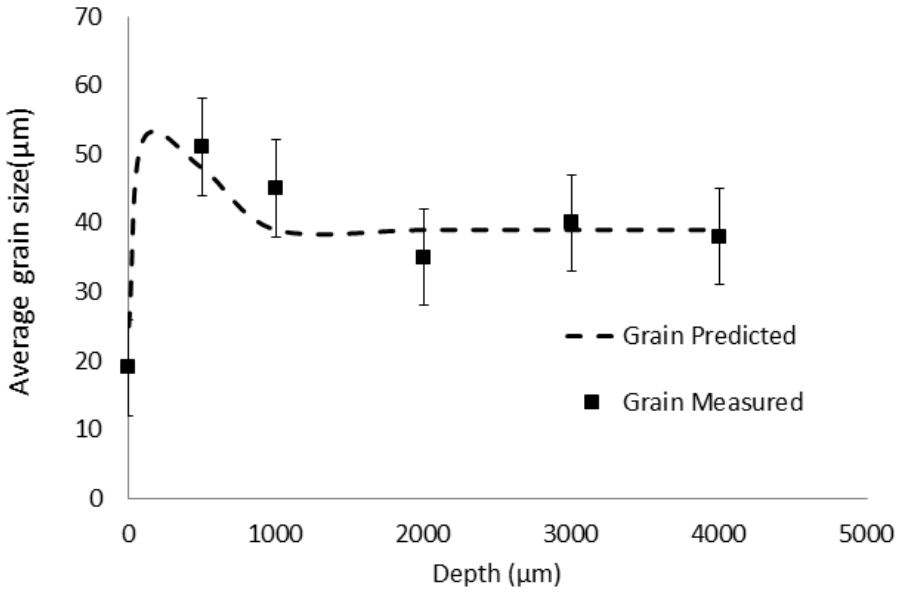

Figure 13: Predicted and measured average grain size in depth (d=0.5 mm, v=3m/s, α= 8°).

3.4 INFLUENCE OF PROCESS PARAMETERS ON THE AVERAGE GRAIN SIZE

Thanks to the machining process signature section it is possible to investigate the effect of the process parameters on the average grain size of the machined surface. Therefore, the effect of the rake angle, cutting speed or even the depth of cut can be investigated using the validated model presented in the previous section. Using the proposed model it is therefore possible to optimize the machining cutting conditions and tool geometry in order to achieve a desirable surface grain size. A very recent work was proposed in order to capture the effect of machining condition on the microstructure [48]. This model was based on a dislocation dynamics physics model.

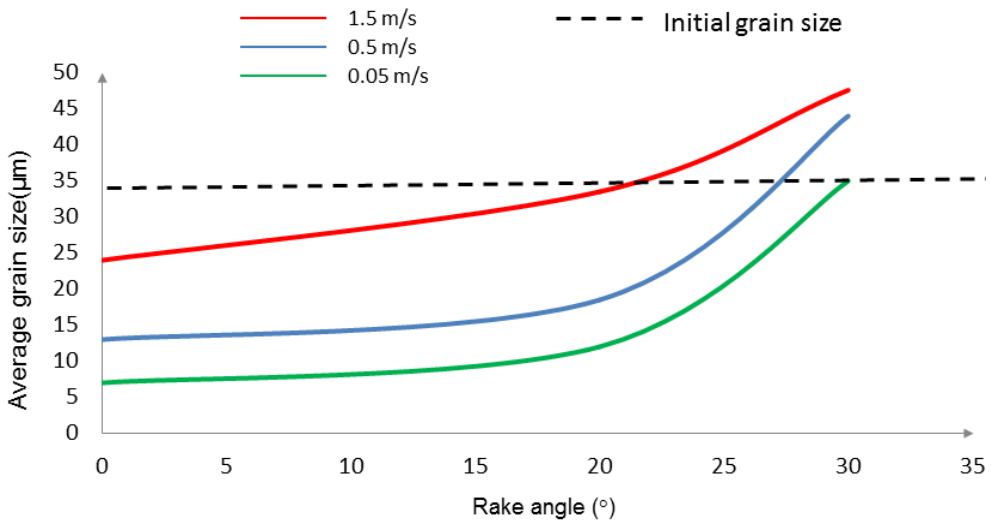

Figure 14: Effect of rake angle on average grain size at different cutting speeds.

Based on the simulated results the different process parameters are affecting the surface average grain size. In fact, regarding the tool geometry, it is known that the shear strain as one of the primary parameter is depending on the rake angle. Increasing the rake angle will have less effect on the grain size. The smaller the rake angle, the more refinement is observed Figure 14). However, while increasing the cutting speed, the increase of the cutting temperature can therefore affect the rake

angle effect on the grain size. Hence, it is important to observe the effect of the cutting speed on the grain size.

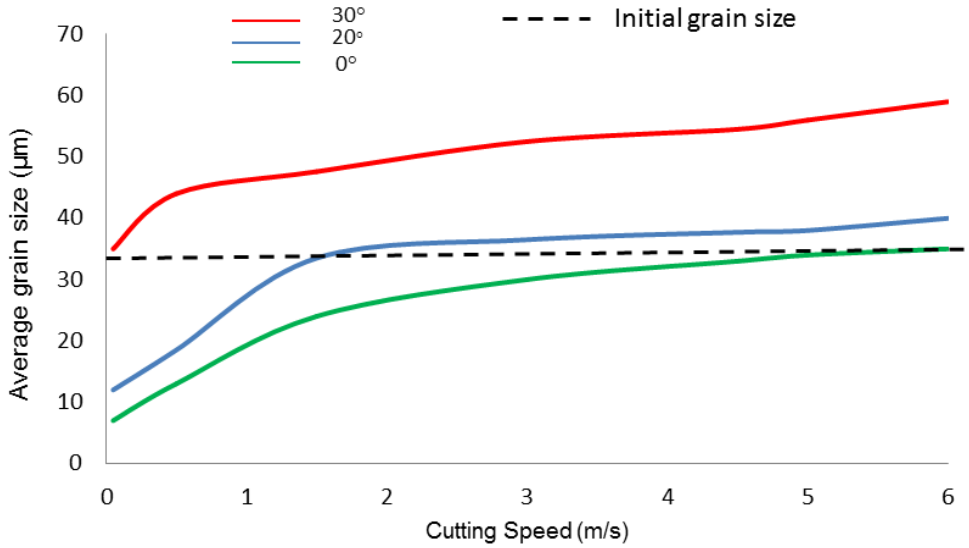

Figure 15: Effect of cutting speed on average grain size at different rake angles values.

The cutting speed as the rake angle is a critical parameter in order to capture the process mechanics and especially the shear strain. While increasing the cutting speed, the increases of the cutting temperature and the strain rate will affect the dynamics recrystallization. From a critical value around 2 m/s, the grain refinement will be very weak Figure 15). However, at a very high rake angle, the refinement won't be observed.

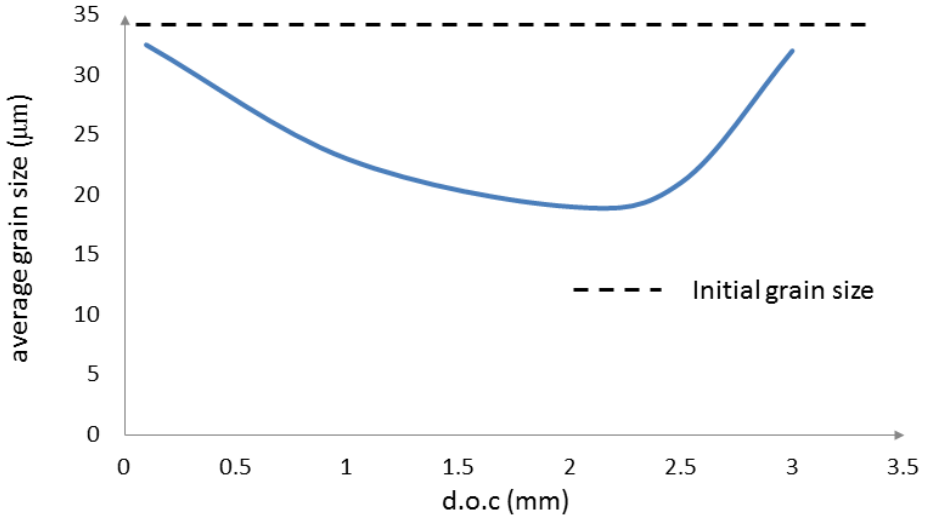

Figure 16: The effect of the depth of cut on the average grain size at constant rake angle and cutting speed.

The depth of cut as independent parameter will affect the process mechanics. As we increase the cutting depth of cut the cutting forces are increasing. Hence, it is expected that this parameter can affect the average grain size on the machined surface. In fact, before 2mm depth of cut, and at a constant speed and rake angle, the grain will observe a refinement. However at higher depth of cut, the extreme cutting forces and temperature will activate grain growth and stop the nucleation dynamics Figure 16).

3.5 CONCLUSION

The importance of the microstructure evolution during the machining process is fundamental to understand in order to achieve desirable functionalities. The materials properties are in fact affected by the microstructure, especially the grain size. In this study, a new approach to predict the grain size on the machined surface is introduced by superposing two simultaneous mechanisms: Grain growth and refinement. This approach considers the grain refinement due to dynamic recrystallization as well as the observed grain growth due to the machining temperature. The dynamic

recrystallization induced by the severe plastic deformation on the chip and part of the surface was captured using the well-known Zener-Hollomon parameter. The observed grain growth attributed to temperature was in this study captured based on a thermal diffusion growth model. The linear superposition of this two method lead to a good prediction of the final average grain size. The advantage of this method is that it can be used on different machining configuration depending on the cutting process parameters. This was demonstrated on two machining cases: the first experiment on AA7075 aluminum alloy with high machining temperature and the second one on a machining of AA6061 with conservative cutting conditions in order to avoid the machining temperature. The experimental validations offered the possibility to validate the average grain size as a depth profile. The experimental results were also useful in order to separate the mechanical and thermal effect. Further, the effects of process parameters on the average grain size were investigated.

CHAPTER IV

TEXTURE EVOLUTION IN MACHINING PROCESS

4.1 INTRODUCTION

Texture is defined as the distribution of crystallographic orientations of a polycrystalline material. We say there is no texture when these orientations are fully random. If there is preferable orientation, we say there is texture. Texture can be weak, moderate or strong. Texture is observed in almost all engineered materials and depends strongly on the manufacturing process. A Solid with a perfectly random texture is called isotropic, in a perfect single crystal is strongly anisotropic. This means that the properties are changing depending on the direction. In many materials, properties are texture-specific, and development of unfavorable textures when the material is fabricated or in use can create weaknesses that can initiate or exacerbate failures. Here, it is clear that texture of a material is a critical attribute that need to be understood during the engineering or a materials or at the manufacturing level, the production of a component. It have been reported in different studies how manufacturing process such as rolling or extrusion are affecting the texture [49] [50] especially in new materials such as Magnesium. An evolution from random or weak texture was always changed to strong preferred orientation. Recent studies investigated the effect of different parameters on the texture. The effect of the materials composition and type of crystal structure was investigated. How the plastic deformation is affecting the texture of the machined surface. How machining compare to other well understood processes. Finally, a method based on a crystal plasticity model is proposed in order to predict the texture evolution in the machining process

for the first time. Experimental investigations using X-ray technic are performed in order to compare the simulated and predicted data.

4.2 VISCOPLASTIC SELF-CONSISTENT MODEL

The Viscoplastic Self-Consistent (VPSC) approach is inspired by the early work of Hill [25] on the self-consistent theory and later developed into a substantial scheme of texture evolution prediction for large inelastic deformations [27] [51] and been recently modified for different materials systems and conditions [52] [53]. The self-consistent approach assumes each grain is an anisotropic ellipsoidal Eshelby inclusion embedded in homogeneous equivalent medium (HEM) as shown in Figure 17**)**

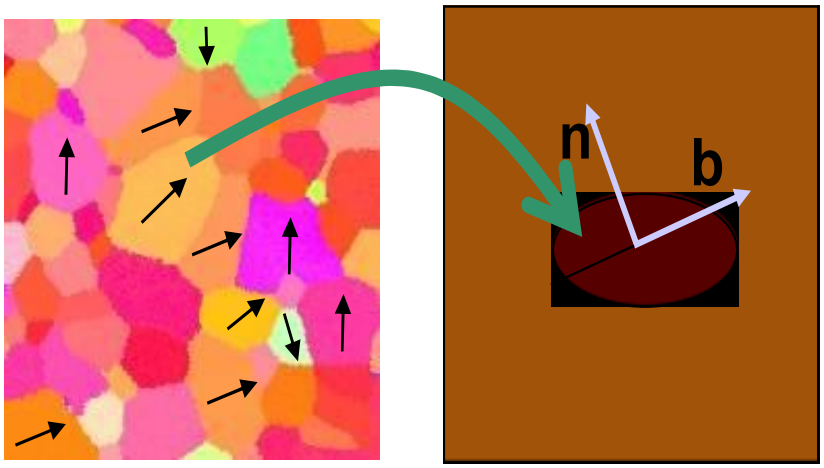

Figure 17: Eshelby's ellipsoidal inclusion assumption.

The difference from Eshelby's approach [53] is the non-linear interaction between strain and stress. The HEM is represented by the polycrystalline aggregate. The consistency condition requires the volume average of the local fields be equal to macroscopically applied fields. Obviously, the HEM should possess uniform properties. The kinematic interaction equation that relates the strain rate and stress in the grain is:

$$\dot{\varepsilon}'_{ij} = \dot{\gamma}_0 \sum_s m^s{}_{ij} \left(\frac{m^s : \sigma'}{\tau^s}\right)^n = M_{ijkl}\sigma'_{kl} \tag{3}$$

where s denotes the slip system of the crystal. $\dot{\gamma}_0$ represents a reference shear rate. $m^s{}_{ij} = b_i{}^s n_j{}^s$ is the geometric Schmid tensor and $\mathbf{n}^s$ and $\mathbf{b}^s$ are respectively the slip plane normal and slip plane direction for the slip system s. τ^s is the critical stress controlling the activation of the slip system and n is the inverse of rate sensitivity. σ' designates the deviatoric stress tensor. Assuming the following equation holds in the HEM:

$$\dot{\bar{\varepsilon}}'_{ij} = \bar{M}_{ijkl}\bar{\sigma}'_{kl} \tag{4}$$

A bar on the top of symbols denotes the macroscopic quantities. The 4th rank tensor $\bar{\mathbf{M}}$ is the compliance of the HEM and relates macroscopic strain rate to macroscopic deviatoric stress.

Therefore, one can prove [16]:

$$\dot{\varepsilon}'_{ij} - \dot{\bar{\varepsilon}}'_{ij} = -\tilde{M}_{ijkl}(\sigma'_{kl} - \bar{\sigma}'_{kl} \tag{5}$$

where the 4th rank tensor $\tilde{\mathbf{M}}$ is the interaction tensor and is equal to:

$$\tilde{M}_{ijkl} = (\boldsymbol{I} - \boldsymbol{S})^{-1}{}_{ijmn} S_{mnpq} \bar{M}_{pqkl} \tag{6}$$

Where $\mathbf{I}$ is the 4th rank identity tensor and $\mathbf{S}$ is the Eshelby tensor [53]. The VPSC procedure as explained elsewhere [52] consists of an initial guess (through Taylor's approach [54]) of the stress tensor in the grain and the iterative solving of the macroscopic compliance tensor and then calculating the stress in each grain from the kinematic interaction equation till the error between the two consecutive values of stress becomes smaller than a tolerance amount. τ^s the critical shear stress is updated by a modified version of the hardening law proposed by Voce [55]:

$$\tau^s = \tau^s{}_0 + (\tau^s{}_1 + \theta^s{}_1\Gamma)\left(1 - \exp\left(-\Gamma\left|\frac{\theta^s{}_0}{\tau^s{}_1}\right|\right)\right) \tag{7}$$

Where Γ is the accumulated shear in the grain. τ_0, τ_1, θ_0 and θ_1 are respectively the initial and asymptotic critical shear stresses and initial and asymptotic hardening rates of the slip system *s*.

The implementation procedure of the VPSC to predict the texture evolution in the orthogonal cutting was achieved following the procedure described in Figure 18**).** In order to accurately capture the materials behavior during the machining process, the strain and stresses history were derived in the case of plain strain machining process.

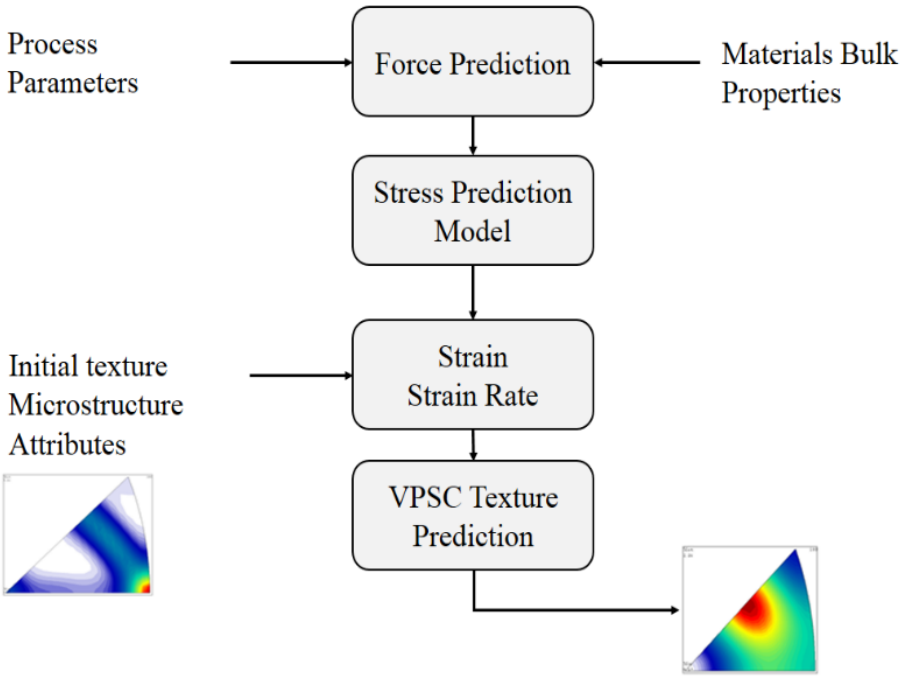

Figure 18: Texture evolution prediction methodology.

It was proven that the deformation history implied by the different deformations and heat treatments have a great influence on the texture. The plastic deformation defined by the plastic strain ε_p. Shear strain based deformation such as machining creates a dislocation motion based on the glide of loops on crystallographic planes. The restricted glides through the deformation volume will generate a uniform shear. Based on the compatibility condition in a solid, it is expected that the shear will produce a

lattice rotation to maintain the grain alignment. In this chapter, the evolution of texture in the machining is investigated using VPSC code from Los Alamos. This crystal plasticity based model is capable of predicting texture evolution based on the deformation velocity gradient as well as the initial texture and other microstructure attributes. It is clear that the deformation generated by the machining has to be clarified in order to implement the right inputs the crystal plasticity model. An approach based on the physics based understanding of the machining deformation is used. The velocity gradient composed of strain rate and spin rate are derived.

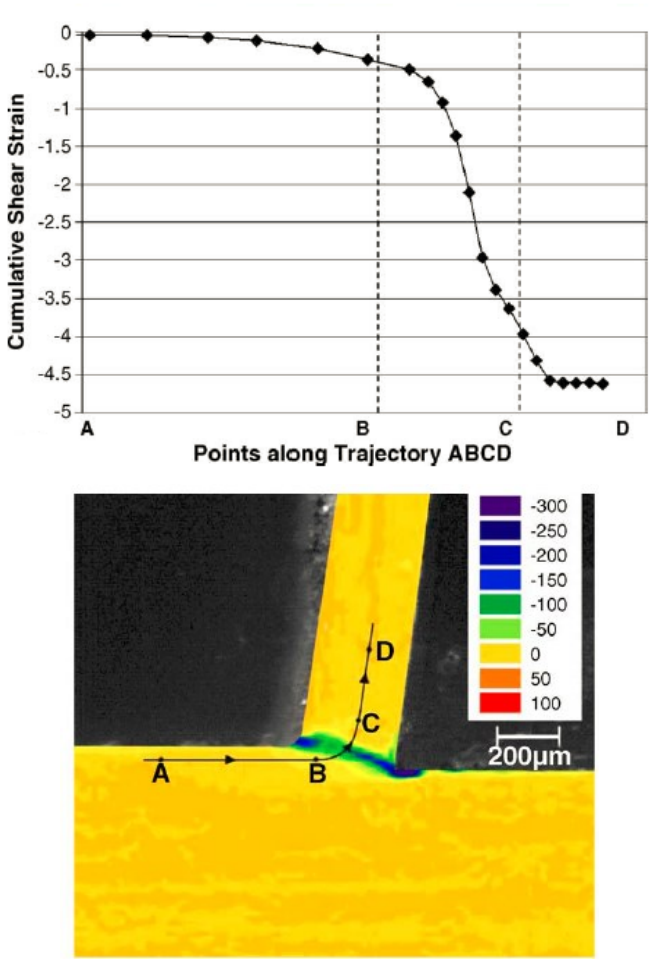

Figure 19: Strain evolution during machining [56].

During the machining cycle, each point will experience an evolution of the strain. In Figure 19), the cumulative shear strain along the trajectory is shown. This trajectory

shows that the strain evolves from zero to a high value in the chip then there is stagnation. The maximum point is happening in the shear plane. However in the workpiece the strain history is slightly different. In fact, the strain and stress will increase and decrease to come back to almost the initial value. Figure 20) shows how the stress magnitude changes during the machining pass. Most importantly, the strain history was also captured as a function of time during the machining process. Strain component in most of the concerned direction can be seen in Figure 21). In this figure, strain over the yy direction is zero based on the plane strain assumption. The other strain components show a similar behavior, which will lead to the deformation gradient needed in this study to capture the texture evolutions.

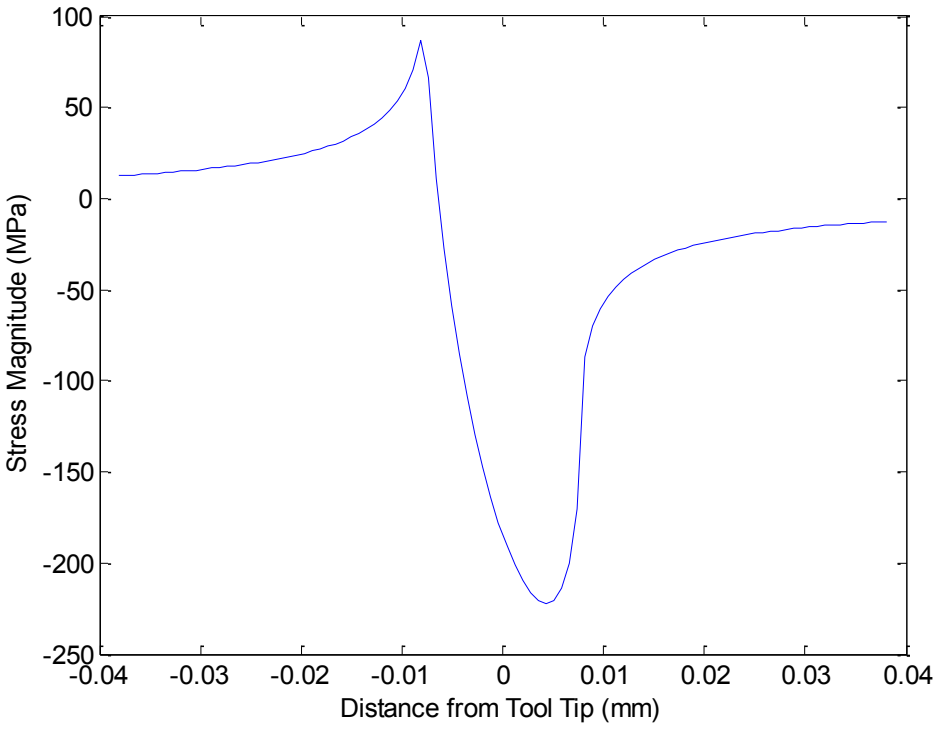

Figure 20: Effective tress evolution during the machining pass.

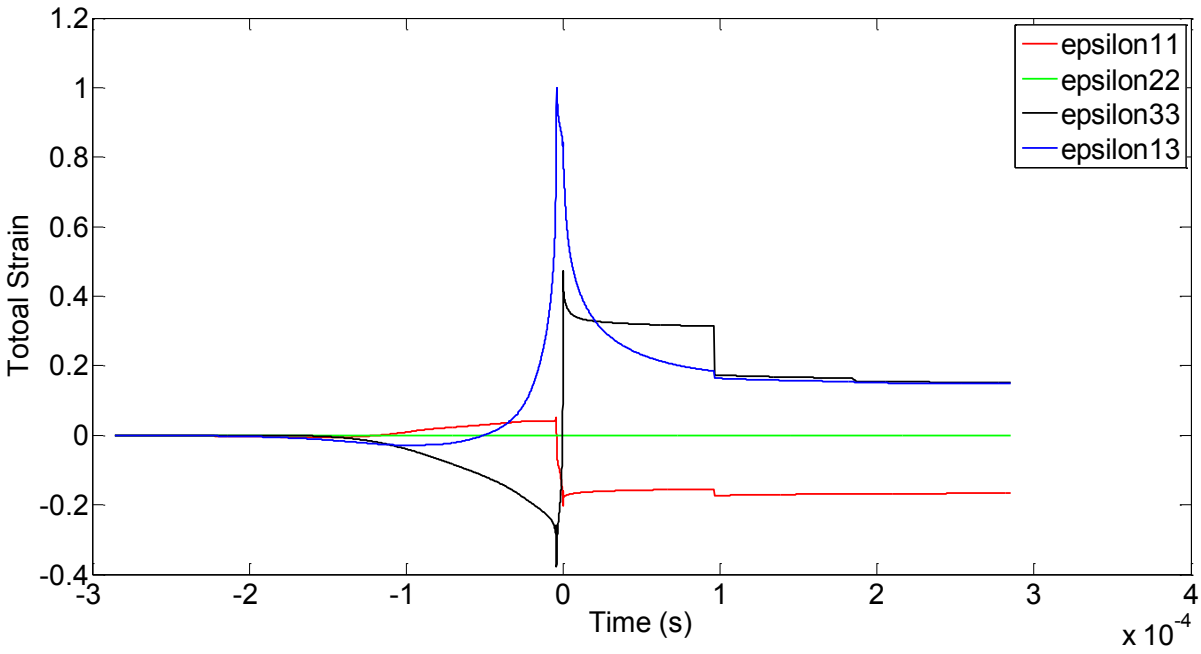

Figure 21: Strain component history during a machining pass.

A multi-step velocity gradient is therefore derived in order to implement the correct strain history experienced by the workpiece during the machining process. It is assumed that the workpiece is stress free and therefore does not present any residual strain. Based on this method, the VPSC simulations were performed to compute in a multi-step manner the texture evolution. The resulting pole figures were plotted using mtex software in matlab. The details of this procedure are proposed in Figure 22.

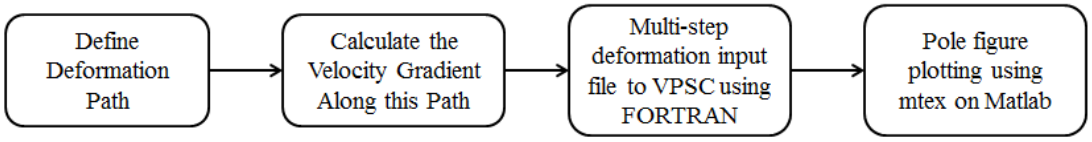

Figure 22: Technical procedure used to predict texture.

4.3 MATERIALS AND EXPERIMENT

The materials system used in this research is aluminum alloy 7075-T651 heat treated, which is widely used for various aerospace applications. The materials properties are

described in Table 1. A CBN cutting insert with a rake angle of 5 ° was used for this experiment. Forces were measured on a multicomponent dynamometer KISTLER type 9257B with a range of [-5, 10] kN mounted on a HARDINGE lathe. Results of predicted and measured cutting forces are presented in Figure 24. A fresh cutting insert was used for each experiment in order to keep the edge radius constant. The tool didn't present any wear.Table 2 summarizes the cutting conditions. The cutting condition where selected as $V = 0.5m/s$ and the width of cut was 3 mm. The effect of depth of cut was investigated by changing it from $0.1mm, 1mm$ and $2mm$. As shown in Figure 23, the initial material properties are attributes of the VPSC algorithm. The workpiece used was rod with a diameter of 3.5 cm. Material microstructure characterization was performed in order to measure the initial grain size and the initial texture before machining. The initial texture and the initial average grain size (45 μm) of the machined rode. The initial texture have shown a strong texture in the [101] direction. This is due to the drawing process used for the fabrication of this specific rod.

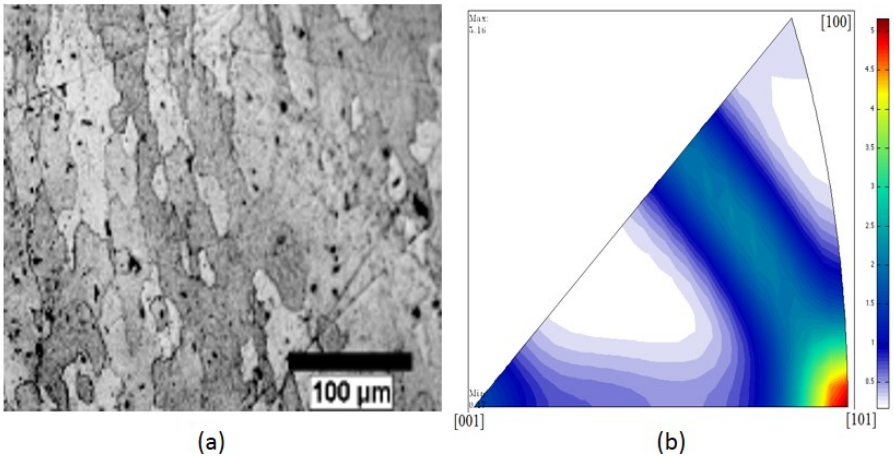

Figure 23: (a) Initial average grain size (b) initial texture distribution.

In this work, the effect of the depth of cut will be investigated. The depth of cut is important independent parameters affecting the tool wear and the productivity of the

process. Although, different previous researches highlighted the fact that depth of cut has a small influence on the evolution of microstructure compared to the rake angle, we propose in this study to see how depth of cut will affect the texture evolution. Since, from a pure mechanistic understanding of machining, higher depth of cut are expected to generate higher cutting forces.

Table 1: Al7075-T651 materials properties.

ρ (g/cc)	γ	E (MPa)	H (HV)	UTS (MPa)
2.81	0.33	71.7	150	572

Table 2: Cutting conditions for orthogonal cutting.

Case	Rake Angle (deg)	Speed (m/s)	Depth of Cut (mm)	Edge Radius (mm)
A	5	0.500	0.1	0.013
B	5	0.500	1.00	0.013
C	5	0.500	2.00	0.013

The pole figures were extracted from x-ray diffraction measurements performed by a Panalytical Xpret PRO XRD machine with a 1.8kW ceramic Cu tube source and a solid state point detector. 0.04 rad Soller slits were used to make sure the x-ray beams are parallel. The textures were obtained by ϕ-scans in the range of 2.5°-357.2° in 0.01° increments. The ψ angle was changed from 0° to 85° in 5° increments. The scans were done at the corresponding 2θ angles of the (111), (200), (220) and (311) peaks of Al-7075. Defocusing and background data of the same peaks were applied to plot the normalized final pole figures.

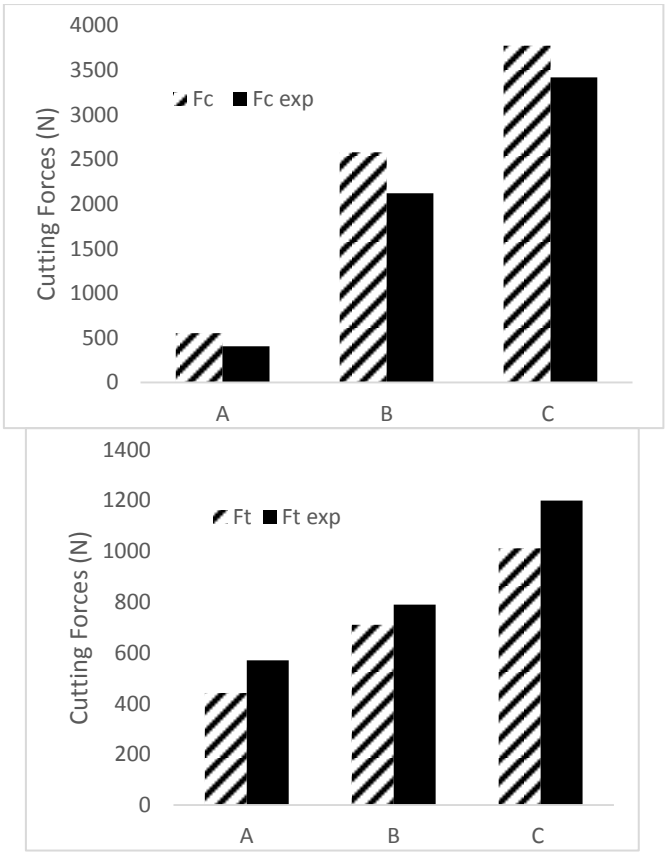

Figure 24: Predicted and measured cutting forces.

4.4 RESULTS AND DISCUSSION

Using the process mechanics approach, deformation velocity, velocity gradient and strain rate tensor associated to each of the cases A, B and C were simulated. The three cases were decided in a way to investigate a large spectrum of possibilities and test the approach for different cutting conditions, from low cutting force to a very large cutting forces configuration as the cutting forces are increasing with the depth of cut. Although the experimental dataset is small, the orthogonal cutting was decided as a test bed realization to investigate the feasibility of the proposed method. After simulations of texture using VPSC and X-ray measurement for the three cases studied in this paper, a comparison is therefore possible based on **Figure 25**, Figure 26 and Figure 27. Both experimental and simulated results are presented on a normalized

scale pole figures in order to make comparison of the direction and magnitude of texture.

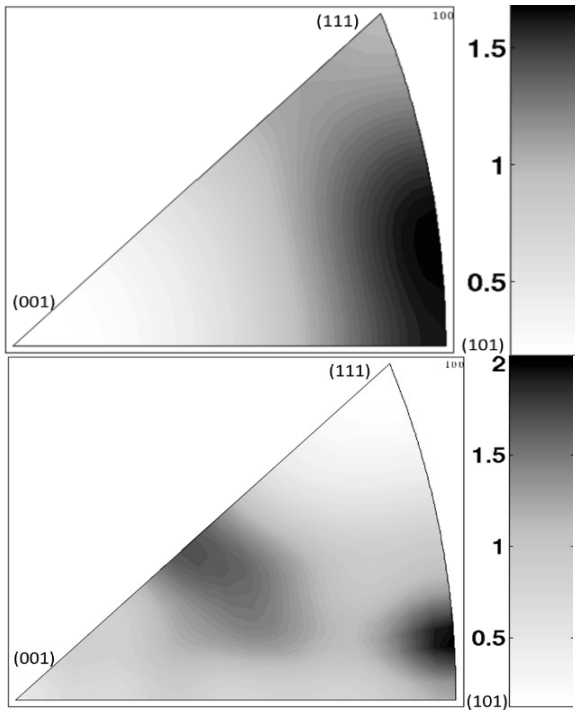

(a) (b)

Figure 25: (a) Simulated texture for case A (b) Experiments for case A.

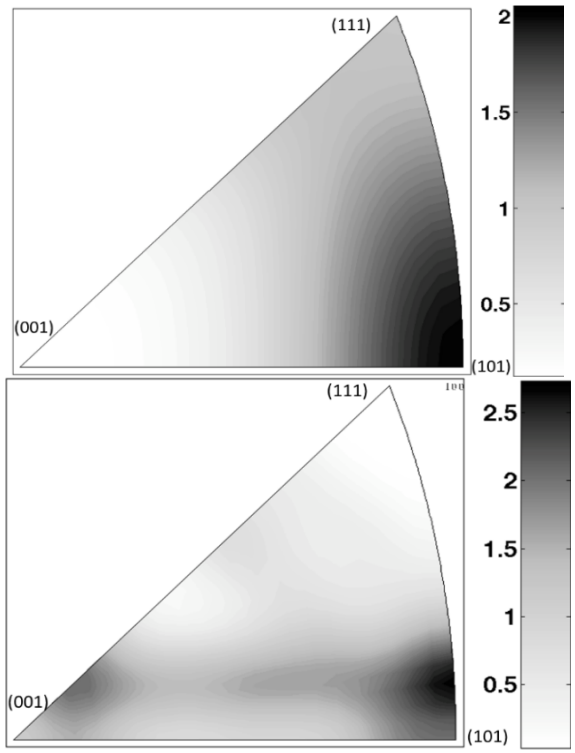

(a) (b)

Figure 26: (a) Simulated texture for case B (b) Experiments for case B.

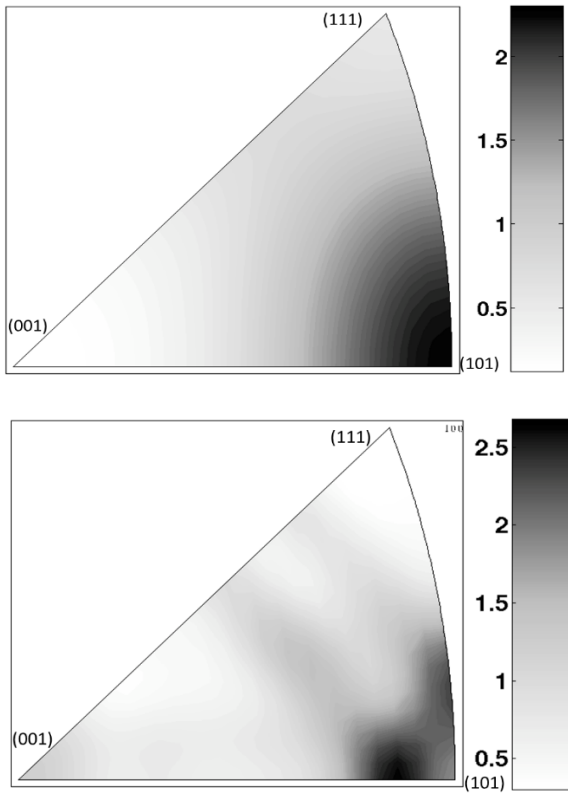

(a) (b)

Figure 27: (a) Simulated texture for case C (b) Experiments for case C.

Based on the comparison between experimental and simulated results, it appears that the VPSC is capable of predicting the concentration of texture on the [101] direction. Prediction shows strong correlations with experimental results. The experimental result shows a dispersed texture at very low depth of cut. The average texture is more and more concentrated on the [101] direction when increasing the depth of cut.

Figure 28 shows a comparison of the magnitude of the texture density at the [101] direction. It is clear that the VPSC predicted linear increases of the magnitude on this direction while increasing the depth of cut. It is believed that the texture of the machined surface will be the same as the shear plane texture [17]. The analytical and the experimental results of this study suggest that the shear induced by the cutting is not the only driving force of the texture. Texture is affected also by the hydrostatic

compression induced by the cutting tip as the input to the VPSC included both aspects of the metal cutting deformation (shear, compression). These changes of the texture magnitude are expected to affect the mechanical properties through the Young's Modulus. On the basis of the results obtained in this study, additional comments with regard to machining forces and therefore the process stability are pertinent. For a given precision machining system, it is known that the cutting forces depends on materials microstructural attributes such as the average grain size of the metal being machined. Based on the results of this work, it is clear that the crystallographic orientation changes during the process will affect the cutting forces. Due to the typical low natural frequencies in the machine tool, chatter might be observed due to these forces variations. It is important to notify that for Aluminum which is an FCC metal, the deformation is favorable in the (111) plane following <101> direction.

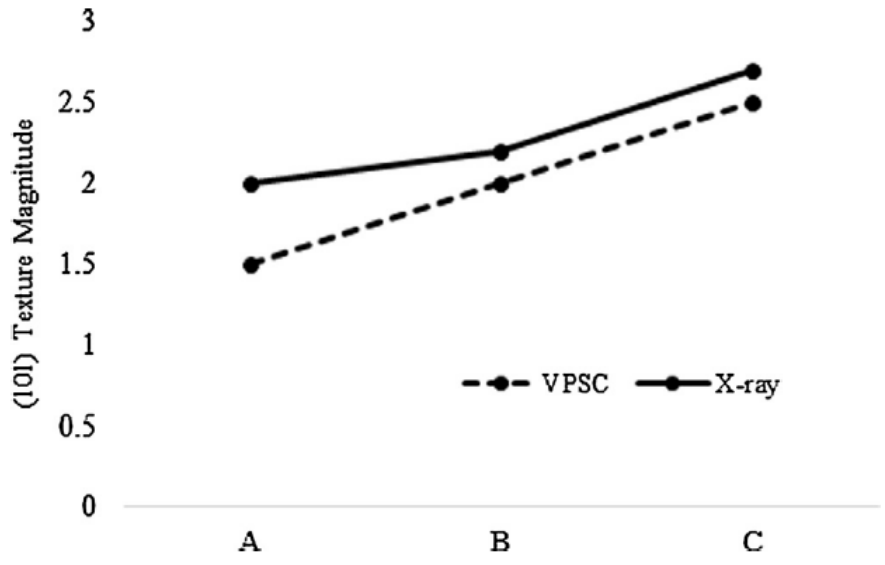

Figure 28: Comparison of predicted and measured magnitude in (101).

4.5 CONCLUSION

This chapter presented a new approach to model and to predict texture evolution in the orthogonal cutting process. A series of analytical and numerical models were

implemented to calculate the forces and therefore the stress, strains, strain rate and velocity gradient. The experiments and simulations agreed that machining processes is inducing a favorable texture and therefore affecting the materials anisotropy. This will lead to an evolution of the mechanical properties of the machined part. This study presents a first step in the exploration of texture evolution during machining processes. In the future, the texture evolution can also be used to predict the bulk mechanical properties resulting from machining. This allows the use of a homogenization procedure with a statistical approach to predict essential materials attributes such as Young's Modulus and therefore the hardness. It is necessary to investigate the reverse problem and understand how the crystallographic orientation changes are expected to affect the machine tool system through the stability analysis. The VPSC approach could be extended to other complex manufacturing processes involving grain level property variations such as laser assisted machining.

CHAPTER V

ANALYTICAL MODEL FOR RESIDUAL STRESS REGENERATION

5.1 INTRODUCTION

The utilization of analytical model to optimize manufacturing process can lead to better manufacturing results especially regarding the prediction of residual stress, distortions and fatigue behavior. The analytical models give a deep physics based understanding of the problem to solve. Regeneration was handled in multi-step loading and unloading situation very accurately due to the simplicity of tension-compression test. In the machining field, multi-step machining can be handled using Finite element modeling. The analytical model capable of predicting residual stress suffered from some weaknesses:

- Large amount of assumptions that affect the accuracy
- No analytical model was capable of predicting residual stress regeneration in the case of multi-steps machining

This step was important in order to bring the analytical models on the same ground as the existing methods used by FEM techniques to solve real engineering problems. The residual stress regeneration can therefore fill the gap and help this technique achieve a maturity level to be capable of being implemented in the production life cycle as shown in Figure 29).

In this chapter, we propose to enhance the exciting mathematical model capable of predicting residual stress. We also propose for the first time an algorithm capable of defining the regeneration problem and solving it using step by step analysis. The

model was validated in the case of multi-step milling process. The experimental results obtained using X-ray were compared to the numerical predictions. The model was capable of predicting accurately the results. The surface residual stress issue was solved thanks to the new enhancement performed in this study.

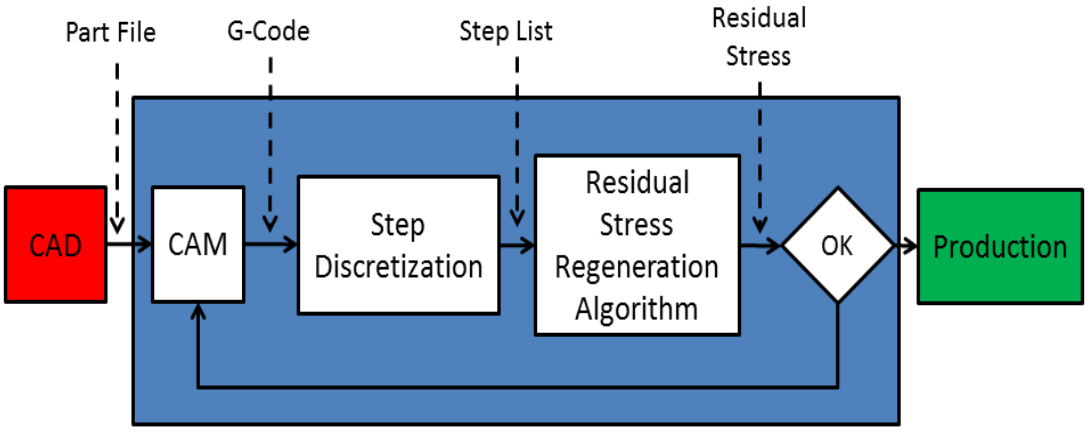

Figure 29: Residual stress regeneration using analytical modeling.

5.2 ENHANCED RESIDUAL STRESS MODEL

Analytical modelling is a powerful tool to predict residual stresses accurately in a very short computational time. Close form solutions are always preferred since they provide a thorough understanding of the physics of residual stresses. In previous published paper some aspects of the modeling of residual stresses in machining was discussed [32]. The proposed model considers different aspects of the machining process. First, the process mechanics equations to predict cutting forces are implemented using [57]. During the machining process, it is known that the process induces a mechanical loading as well as a thermal loading. Theses loadings have to be determined accurately in order to predict the loadings stresses that will be used in the McDowell based model for residual stresses. For this purpose, different models were used in this work to predict the elastic loading as well as the stresses induced by the non-uniform heating.

Different model were proposed in order to predict the temperature in the machining process. For oblique machining a new model based on finite differences was proposed by [58], more traditional models based on the moving heat sources were also proposed. In this thesis we will not focus on the temperature prediction modeling, however, the temperature predicted is used in order to predict thermal stress. In fact, Timoshenko in [59] presented a complete theory of thermal stresses in elastic bodies. In this study, we assume we are in elastic domain. This assumption is valid since in this study we are interested in the section of the workpiece that was not affected by the plastic deformation. In machining the plastic deformation is happening in the shear plane and the chip that is technically removed.

5.2.1 THERMAL PLASTIC STRESSES

It is known that thermal stresses in a semi-infinite body will be the result of the superposition of:

- Stresses due to body force $\mathbf{X} = -\big(\boldsymbol{\alpha}\mathbf{E}/(\mathbf{1}-\boldsymbol{\nu})\big)(\boldsymbol{\delta}\mathbf{T}/\boldsymbol{\delta}\mathbf{x})$ and $\mathbf{Z} = -\big(\boldsymbol{\alpha}\mathbf{E}/(\mathbf{1}-\boldsymbol{\nu})\big)(\boldsymbol{\delta}\mathbf{T}/\boldsymbol{\delta}\mathbf{z})$,
- Stresses due to a tensile surface traction of $\boldsymbol{\alpha}\mathbf{E}\mathbf{T}/(\mathbf{1}-\boldsymbol{\nu})$,
- A hydrostatic pressure of $\boldsymbol{\alpha}\mathbf{E}\mathbf{T}/(\mathbf{1}-\boldsymbol{\nu})$,

In this work, the non-uniform heating induced by the cutting temperature is assumed to be known. The stresses induced by the non-uniform temperature in the workpiece are obtained from the Green functions of stresses due to a point body load. Based on the literature review, the explicit solutions for such Green functions are available for the plane stress and plain strain. As in the machining configuration we are considering the plan strain case. Derivations of this configuration were inspired from the previous work of [60]. Therefore,

$$\sigma_{xx}^{therm} = -\frac{\alpha E}{1-2\nu}\int_{0}^{\infty}\int_{-\infty}^{\infty}\left(G_{xh}\frac{\partial T}{\partial x}(x',z') + G_{xv}\frac{\partial T}{\partial z}(x',z')\right)dx'dz' + \frac{2z}{\pi}\int_{-\infty}^{\infty}\frac{p(t)(t-x)^2}{\left((t-x)^2+z^2\right)}dt - \frac{\alpha ET(x,z)}{1-2\nu} \tag{8}$$

$$\sigma_{zz}^{therm} = -\frac{\alpha E}{1-2\nu}\int_{0}^{\infty}\int_{-\infty}^{\infty}\left(G_{zh}\frac{\partial T}{\partial x}(x',z') + G_{zv}\frac{\partial T}{\partial z}(x',z')\right)dx'dz' + \frac{2z^3}{\pi}\int_{-\infty}^{\infty}\frac{p(t)}{\left((t-x)^2+z^2\right)}dt - \frac{\alpha ET(x,z)}{1-2\nu} \tag{9}$$

$$\sigma_{xz}^{therm} = -\frac{\alpha E}{1-2\nu}\int_{0}^{\infty}\int_{-\infty}^{\infty}\left(G_{xzh}\frac{\partial T}{\partial x}(x',z') + G_{xzv}\frac{\partial T}{\partial z}(x',z')\right)dx'dz' + \frac{2z^2}{\pi}\int_{-\infty}^{\infty}\frac{p(t)(t-x)}{\left((t-x)^2+z^2\right)}dt \tag{10}$$

Where

$$p(t) = \frac{\alpha ET(x,z=0)}{1-2\nu} \tag{11}$$

Hence, we can write:

$$\sigma_{yy}^{therm} = \nu\left(\sigma_{xx}^{therm} + \sigma_{zz}^{therm}\right) \tag{12}$$

and (G_{xh} , G_{xv} , G_{xh} , G_{zh} , G_{xzh} , G_{xzv}) are the plain strain Green's functions, α is the coefficient of thermal expansion, E Young's Modulus and ν Poisson ration for the workpiece material. It is important to notice that the thermal stresses are function of instantaneous temperature at each point of the workpiece. We assume that during the

machining, every point of the workpiece will experience the same temperature gradient. Therefore, we developed a spatial distribution of the thermal stresses. The workpiece materials are assumed isotropic and homogeneous.

5.2.2 MECHANICAL ELASTIC STRESSES

The mechanical loading can be derived as the elastic loading experienced by the workpiece. The cutting force is modeled as a distribution of load with radial and tangential fractions. An oblique transformation is therefore applied to the cutting geometry. The problem is reduced to two dimensions problem. Again, the workpiece is modeled as a semi-infinite, homogeneous, isotropic, elasto-plastic materials exhibiting rate independent, isotropic hardening with a Won Mises yield surface. The plastic modulus is denoted h. Therefore stresses induced by normal compressive forces and tangential traction can be calculated using the following equations:

$$\sigma_x = -\frac{2z}{\pi}\int_{-a}^{a}\frac{p(s)(x-s)^2}{[(x-s)^2+z^2]^2}ds - \frac{2}{\pi}\int_{-a}^{a}\frac{q(s)(x-s)^2}{[(x-s)+z]^2}ds$$

$$\sigma_z = -\frac{2z^3}{\pi}\int_{-a}^{a}\frac{p(s)}{[(x-s)^2+z^2]^2}ds - \frac{2z^2}{\pi}\int_{-a}^{a}\frac{q(s)(x-s)}{[(x-s)^2+z^2]^2}ds \quad (13)$$

$$\tau_{xz} = -\frac{2z^2}{\pi}\int_{-a}^{a}\frac{p(s)(x-s)}{[(x-s)^2+z^2]^2}ds - \frac{2z}{\pi}\int_{-a}^{a}\frac{q(s)(x-s)^2}{[(x-s)^2+z^2]^2}ds$$

Where the span of the integrals $[-a.a]$ as a function of the cutting edge radius, where $\sigma_x, \sigma_z, \tau_{xz}$ are the principle stress components on the plane (xz), a,b are integration boundaries, $p(s) and\ q(s)$ are the normal and tangential pressure induced by the cutting tool on the workpiece.

Finally, mechanical and thermal stresses are added to compute the total elastic stresses experienced by the workpiece. This addition is possible since the uncoupled linear elastic theory is utilized in this case based on the Duhamel-Neumann hypothesis.

$$\sigma_{xx}^{*} = \sigma_{xx}^{mech} + \sigma_{xx}^{therm}, \qquad \sigma_{zz}^{*} = \sigma_{zz}^{mech} + \sigma_{zz}^{therm}$$
$$\tau_{xz}^{*} = \tau_{xz}^{mech} + \tau_{xz}^{therm}, \qquad \sigma_{yy}^{*} = \sigma_{yy}^{mech} + \sigma_{yy}^{therm} - \alpha E T \tag{14}$$

5.2.3 MODIFIED MCDOWELL RESIDUAL STRESS MODEL

However, these models are built based on different assumptions that affect the accuracy in some cases. The model introduced by McDowell and used in the case of orthogonal cutting by [31] showed a very good capacity to predict residual stresses in depth. However, this model showed limitations in predicting surface residual stress. It appears that the normal stress σ_{zz} normal in direction to the machining surface and $\dot{\tau}_{xz}^{*}$ were considered as elastic. It is known that in processing like machining, the surface experience a severe plastic deformation with strain from 1 to 10 and strain rate in the order of 10^{9} s^{-1}. We believe that correcting this assumption by considering the plastic aspect of the machining operation and therefore of the normal stress to the machining surface will enhance the accuracy of the model, especially the surface residual stresses that play a key role in the functionality of the manufactured part. For this, it is known that the total strain will be a sum of elastic and plastic strains as shown in Equation (15).

$$\varepsilon_{ij} = \varepsilon_{ij}^{e} + \varepsilon_{ij}^{p} \tag{15}$$

In this study, a plan strain configuration is assumed, therefore the $\varepsilon_{yy} = 0$. Metal in plastic deformation verify the volume invariance described in Equation (16).

$$\dot{\varepsilon_{xx}} + \dot{\varepsilon_{zz}} = 0 \tag{16}$$

Plastic strain rate can be written as Equation (17). <> is the MacCauley brackets, and $\dot{S}_{kl}$ the deviatoric stress increment, n_{kl} component of unit normal in the direction of plastic strain rate and can be written as a function of the back stress α_{ij} as described by Equation (18).

$$\begin{cases} \dot{\varepsilon}^p_{xx} = \dfrac{1}{h}\langle \dot{S}_{kl} n_{kl} \rangle n_{xx} \\ \dot{\varepsilon}^p_{zz} = \dfrac{1}{h}\langle \dot{S}_{kl} n_{kl} \rangle n_{zz} \end{cases} \tag{17}$$

$$\begin{cases} n_{xx} = \dfrac{S_{xx} - \alpha_{xx}}{\sqrt{2}k} \\ n_{zz} = \dfrac{S_{zz} - \alpha_{zz}}{\sqrt{2}k} \end{cases} \tag{18}$$

After substitution of these equation in Equation (16), we can conclude and due to the strict positivity of $\langle \dot{S}_{kl} n_{kl} \rangle$ that $n_{xx} + n_{zz} = 0$. This will systematically lead to $S_{xx} + S_{zz} = 0$. Based on the definition of deviatoric stresses, given by:

$$\begin{cases} S_{xx} = \sigma_{xx} - \dfrac{1}{3}\left(\sigma_{xx} + \sigma_{yy} + \sigma_{zz}\right) \\ S_{zz} = \sigma_{zz} - \dfrac{1}{3}\left(\sigma_{xx} + \sigma_{yy} + \sigma_{zz}\right) \end{cases} \tag{19}$$

Therefore we can conclude that:

$$\sigma_{xx} - \tfrac{1}{3}\left(\sigma_{xx} + \sigma_{yy} + \sigma_{zz}\right) + \sigma_{zz} - \tfrac{1}{3}\left(\sigma_{xx} + \sigma_{yy} + \sigma_{zz}\right) = 0 \tag{20}$$

Then the new condition on normal stresses in term of stress rate can be written as:

$$\dot{\sigma}_{yy} = \frac{1}{2}(\dot{\sigma}_{xx} + \dot{\sigma}_{zz}) \tag{21}$$

This condition can be directly derived from the plane strain assumption and the isochoric aspect of the plastic deformation. In this study we proved this through rigorous derivations.

This new elastoplastic relationship between the three normal stresses is written in it incremental form, and added to the incremental residual stress model in order to satisfy the plastic aspect of the stress orthogonal to the machined surface. This model therefore includes three equations for three unknowns. Compared to the original McDowell's model, this model correct the elastic assumption made to the model regarding $\dot{\sigma}_{zz}$. It is noteworthy to say that the shear stress $\dot{\tau}^*_{xz}$ however in the first equation is still assumed elastic. A relaxation procedure is applied upon these stresses. The relaxation details can be found in [31].

$$\begin{cases} \dot{\varepsilon_{xx}} = \frac{1}{E}\left[\dot{\sigma}_{xx} - v\left(\dot{\sigma}_{yy} + \dot{\sigma}_{zz}\right)\right] + \frac{1}{h}\left(\dot{\sigma}_{xx}n_{xx} + \dot{\sigma}_{yy}n_{yy} + \dot{\sigma}_{zz}n_{zz} + 2\dot{\tau}^*_{xz}\right. \\ = \varphi\left(\frac{1}{E}\left[\dot{\sigma}^*_{xx} - v\left(\dot{\sigma}_{yy} + \dot{\sigma}^*_{zz}\right)\right] + \frac{1}{h}\left(\dot{\sigma}^*_{xx}n_{xx} + \dot{\sigma}_{yy}n_{yy} + \dot{\sigma}^*_{zz}n_{zz} + 2\dot{\tau}^*_{xz}n_x\right.\right. \\ \dot{\varepsilon_{yy}} = \frac{1}{E}\left[\dot{\sigma}_{yy} - v(\dot{\sigma}_{xx} + \dot{\sigma}_{zz})\right] + \frac{1}{h}\left(\dot{\sigma}_{xx}n_{xx} + \dot{\sigma}_{yy}n_{yy} + \dot{\sigma}_{zz}n_{zz} + 2\dot{\tau}^*_{xz}n_x\right. \\ \dot{\sigma}_{yy} = \frac{1}{2}(\dot{\sigma}_{xx} + \dot{\sigma}_{zz}) \end{cases} \quad (22)$$

Where, E is the elastic moduli, h the plastic moduli, φ the blending function and ν the poisson ratio. $\dot{\sigma}_{xx}, \dot{\sigma}_{yy}, \dot{\sigma}_{zz}$ are the relaxed stress increment of normal direction xx, yy and zz. While $\dot{\sigma}^*_{xx}, \dot{\sigma}^*_{zz}, \dot{\tau}^*_{xz}$ are the incremental form of the loading elastic stresses.

The stress increments in x and z direction are integrated in order to find the residual stresses. A relaxation procedure is applied upon parameters until they fulfil the boundary condition. This new equation is used in this study for the residual stress prediction for multi-step machining process. As it is shown in the next section, the surface residual stress results were enhanced drastically.

The constitutive equations are described in Table 3.

Table 3: Constitutive equations used in the model.

Equation Description	Equation
Von Mises yield surface	$F = \frac{3}{2}\left(S_{ij} - \alpha_{ij}\right)\left(S_{ij} - \alpha_{ij}\right) - R^2 = 0$
Deviatoric stress	$S_{ij} = \sigma_{ij} - \left(\sigma_{kk}/3\right)\delta_{ij}$
Plastic strain rate (normality flow rule)	$\boldsymbol{\varepsilon_{ij}^{p} = \frac{1}{h}\langle S_{kl} n_{kl}\rangle n_{ij}}$
Components of unit normal in plastic strain rate direction (on yield surface)	$n_{ij} = \frac{S_{ij} - \alpha_{ij}}{\sqrt{2}k}$
Evolution of back stress for linear kinematic hardening	$\boldsymbol{\dot{\alpha}_{ij} = \langle \dot{S}_{kl} n_{kl}\rangle}$

It is expected that during the multi-step machining process, a nonproportional cyclic plasticity will be experienced by the workpiece. A multiple back stress nonlinear dynamic recovery constitutive law was integrated to capture the cyclic plasticity generated by the cutting process. More details about the constitutive law can be found in [61]

5.3 REGENERATION ALGORITHM

The residual stress regeneration was solved for manufacturing operation such as multi-cycle rolling [61]. For metal cutting, the mechanisms behind are different. The fact of eliminating a layer implies that residual stress will mainly regenerate based on a reduced profile as the depth of cut will eliminate a layer of it. Phenomena like cold working due to the kinetic hardening are not dominant. In order to solve this issue, a comprehensive algorithm is designed as shown in Figure 30). The process parameters as well as the initial condition regarding the pre-exciting residual stress field are

introduced. For simplification purpose, the initial residual stress is none exciting. Based on these inputs and using the model described in Equation (20) it is possible to predict the residual stress field in the workpiece. If there is another machining step, predicted residual stress field is updated using the new depth of cut using Ep (8). Figure (4) shows the elimination process in a schematic manner. The reduced stress field become therefore a new initial condition used in the Equation (23) to predict the new residual stress field. This operation is conducted iteratively until the last machining step.

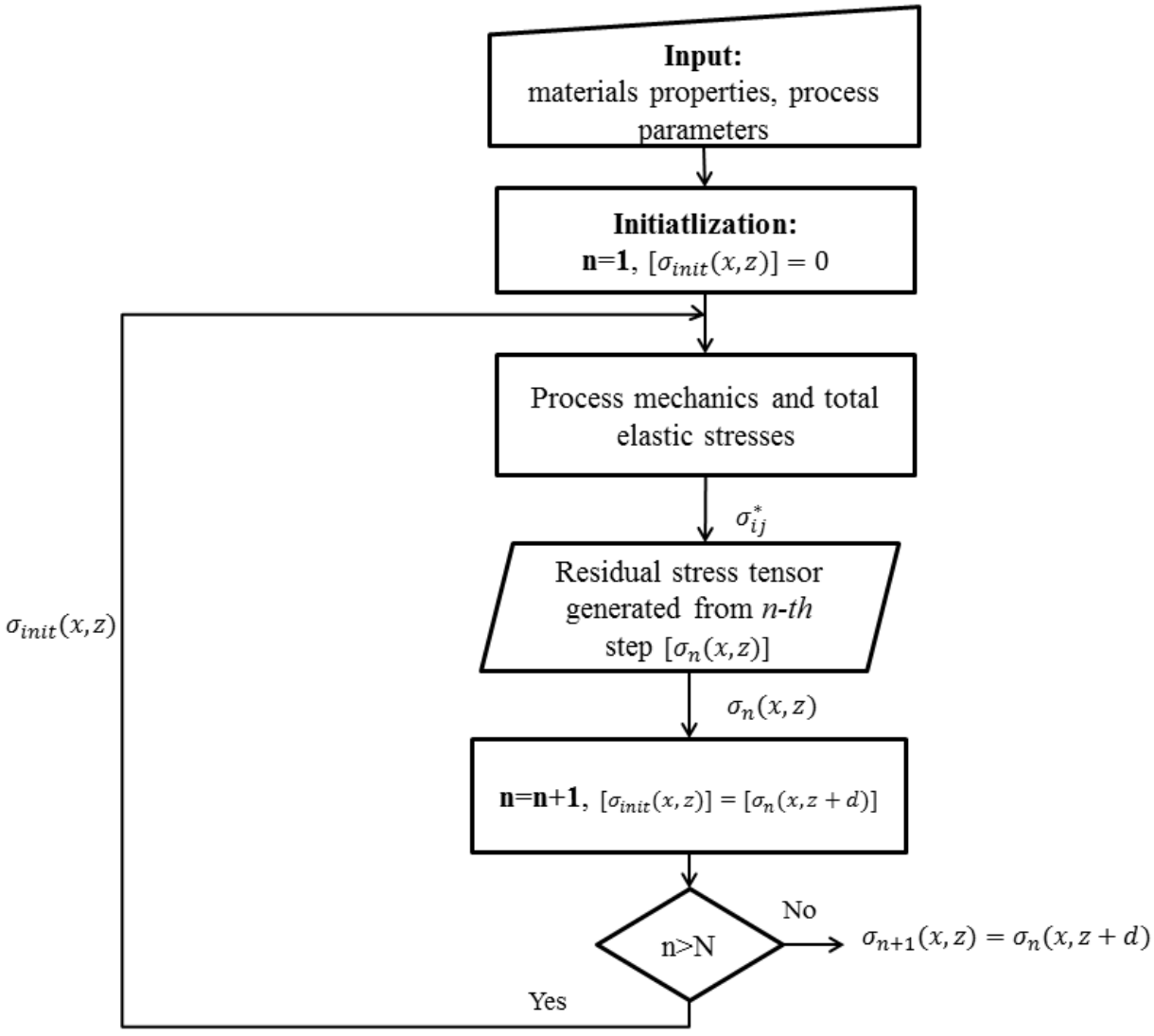

Figure 30: Flowchart for residual stress regeneration algorithm.

The elimination procedure is an important step as it is used to generate the initial condition to be used in the model in order to predict the residual stresses. Equation (23) describes how the depth of cut is used to update the residual stress field after the cut is achieved.

$$\begin{cases} \sigma_{xx}^{n+1}(x,z) = \sigma_{xx}^{n}(x,z+d) \\ \sigma_{yy}^{n+1}(x,z) = \sigma_{yy}^{n}(x,z+d) \end{cases} \quad (23)$$

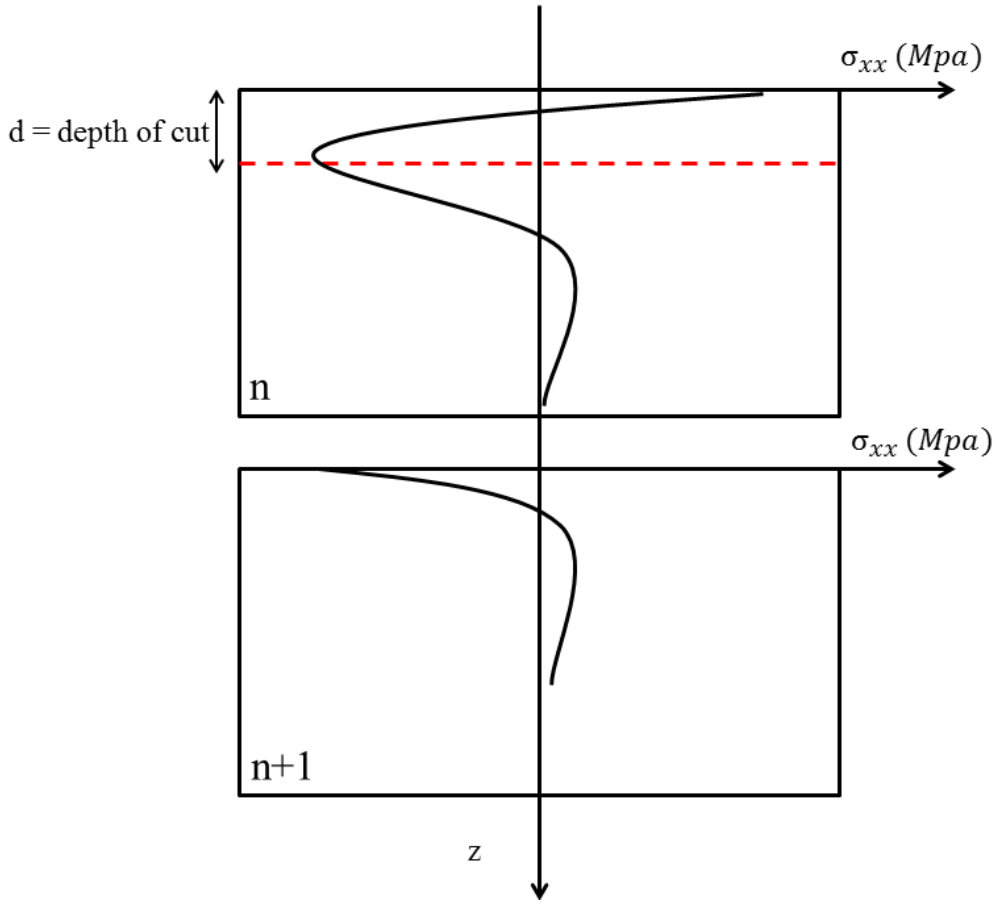

Figure 31: Elimination of residual stress due to machining step.

The elimination procedure is described in Figure 31). The obtained stresses are therefore used in Equation 21 as an exciting stress field (i.e initial condition) that will contribute to the prediction of the final residual stress profile. The effect of temperature on the residual stress relaxation is assumed as negligible in this study.

Later on in the experimental part this assumption will be discussed. It is expected that during the multi-step machining process, the workpiece undergoes non-proportional cyclic plastic deformation. Hence, a multiple back-stress nonlinear dynamic recovery constitutive law was integrated to capture the cyclic plasticity generated by the cutting process: The back-stresses are calculated using Equation (24)

$$\dot{\alpha_{ij}} = \langle \dot{S_{kl}} n_{kl} \rangle n_{ij} \tag{24}$$

where S_{kl} is the deviatoric stress and n_{kl} stand for the normal vectors.

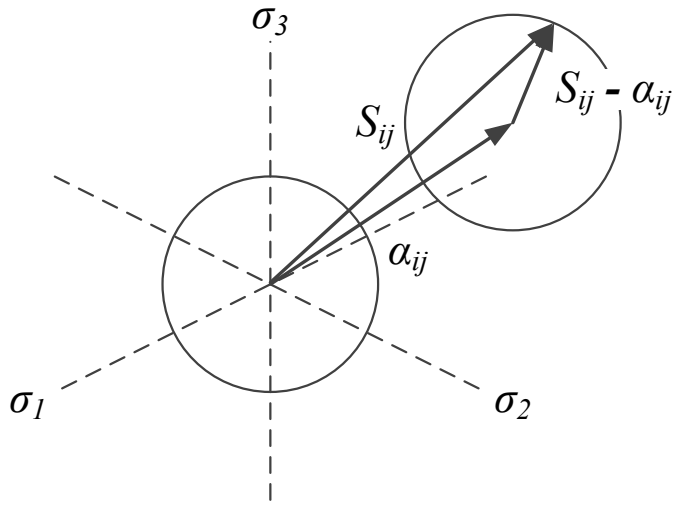

Figure 32: Schematic of back stress effect on the yield surface.

More details about the constitutive law formulation can be found in [61]. The back-stress is changing after each machining step and will consequently affect the residual stress regeneration, as illustrated by the figure. After each loading and unloading operation the yield surface is shifting by α_{ij} how the yield surface is changing after each machining step in Figure 32) by a translation of α_{ij}.

5.4 Material and experiment

In order to validate the proposed model, milling of milling of AA2024-T3 was performed on Bridgeport machine (model XR1000). The aluminum alloy is used in

automotive industry and have the following composition (Al 93.5%, Cu 4.4%, Mg 1.5%, Mn 0.6%). The material properties were measured as (E=73 GPa, ν=0.3, ρ=2780kg/m^3, UTS= 427 MPa, σ_{yield}= 276 MPa). A carbide grade end-mill tool with a diameter of 6mm was used. It has 4 flutes and a rake angle of 15° a clearance angle of 6° and a helix angle of 30 °. Tool was fresh. Figure 33) shows the used experimental setup for the milling operation.

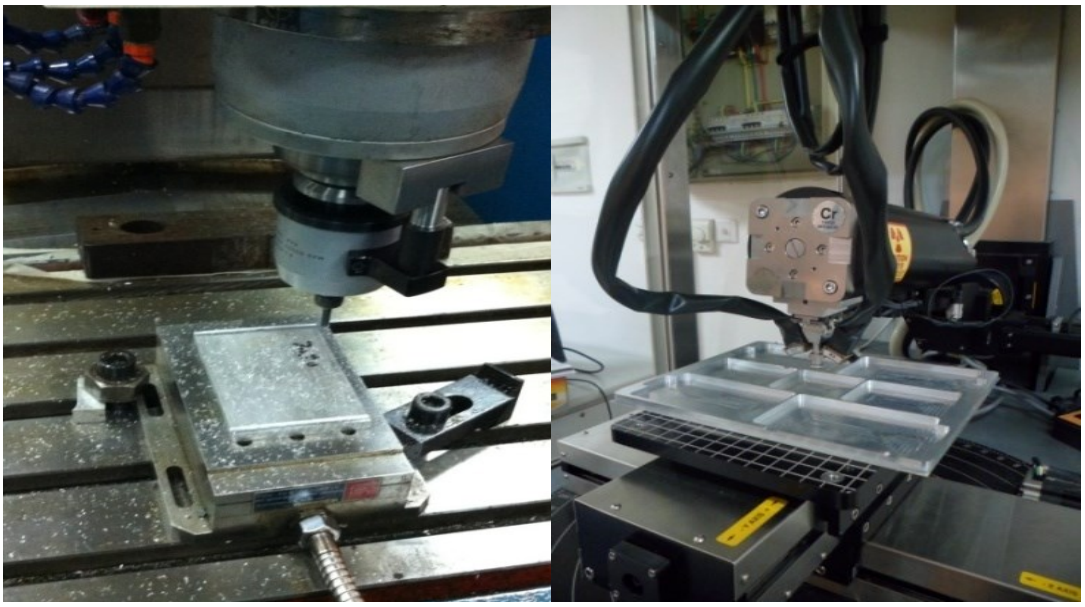

(a) (b)

Figure 33: (a) Machining setup (b) X-ray measurement setup.

The machining operation followed the procedure described in Table 4. Successive operations following the industrial standards were selected in order to investigate the regeneration of residual stresses. The operation started by roughing and ended with finishing. Continuous cooling was applied in order to avoid an important temperature rise in order to support the assumption that no relaxation will be observed. In order to investigate the residual stresses in depth, X-ray measurement were performed. A high-power Canada PROTO residual stress analyzer (LXRD) was used as shown in Figure 33). The X-ray machine had a Cr target with a voltage of 25 KV. The AA2024-T3 alloy had a Bragg angle 2θ of 156.31°, a diffracting plane (222). Electro-

polishing operation was performed using a PROTO 8818-V2 in order to eliminate materials layers to observe residual stress in depth. The electro-polishing material removal rate was determined experimentally. Polishing five seconds on flat surface of the part with voltage of 100VDC and flow rate of 10mm^3/min will remove a layer of 37 μm.

Table 4: Processing schedule and process parameters.

	Procedures	Milling speed V [rev/min]	Feed rate f [mm/tooth]	Depth of cut a_p[mm]
Processing parameters	Roughing	3500	0.1	0.5,0.2,0.1
	Finishing	3500	0.05	0.08,0.025,0.01

For comparison purpose, it is necessary to make sure the initial residual stress profile is uniform and close to zero. Stress relieve heat treatment was performed for this purpose. The initial material was heated to 495° then kept warm for 80 min, then quenched in water at 20°. After this first step, the raw material was again kept warm at 195° for 12h, and then cooled to room temperature. The stresses before and after the stress relieve treatment can be seen in Figure 34.

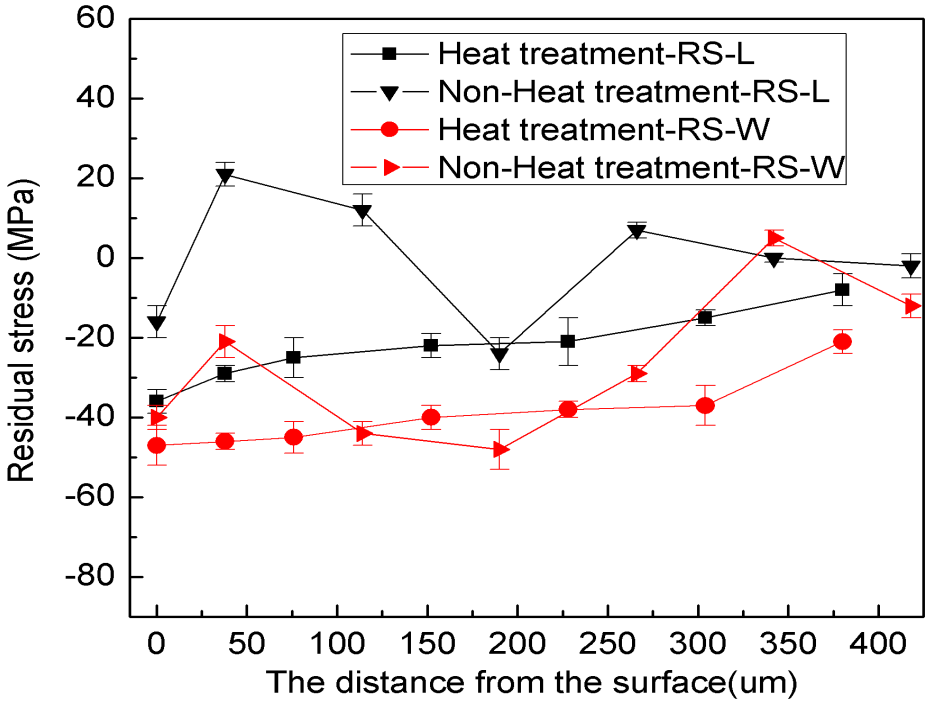

Figure 34: Stress relief heat treatment results.

5.5 RESULTS AND DISCUSSION

The elastic theory was used to derive the mechanical and thermal loading induced by the machining forces and temperature. The elastic stresses were added in a uncoupled manner using the linear elastic theory as presented in the section before. Using the enhanced model, simulations were performed in order to predict residual stresses in millings at the specific case of regeneration. Residual stresses in the transverse and the cutting direction are therefore computed. Figure 35) and Figure 36) shows a comparison of the simulated and measured residual stress profile for each machining step. Error! Reference source not found. presents the experimental and simulated data rom the other parameters.

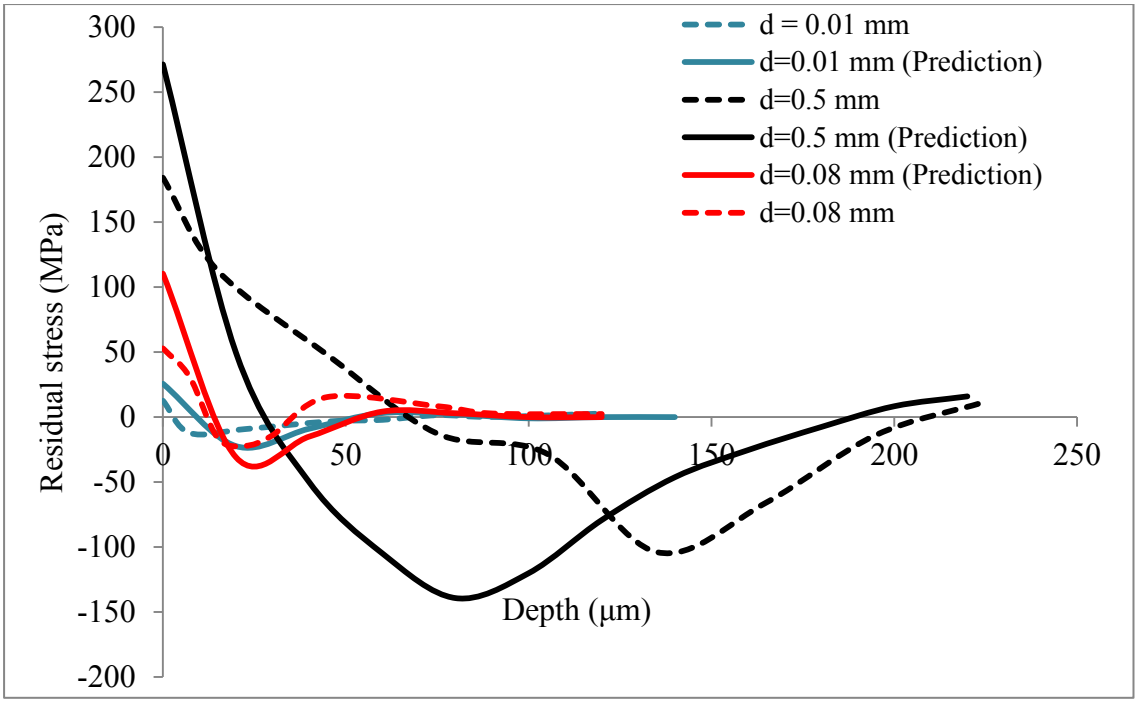

Figure 35: Predicted and experimental residual stress in X direction.

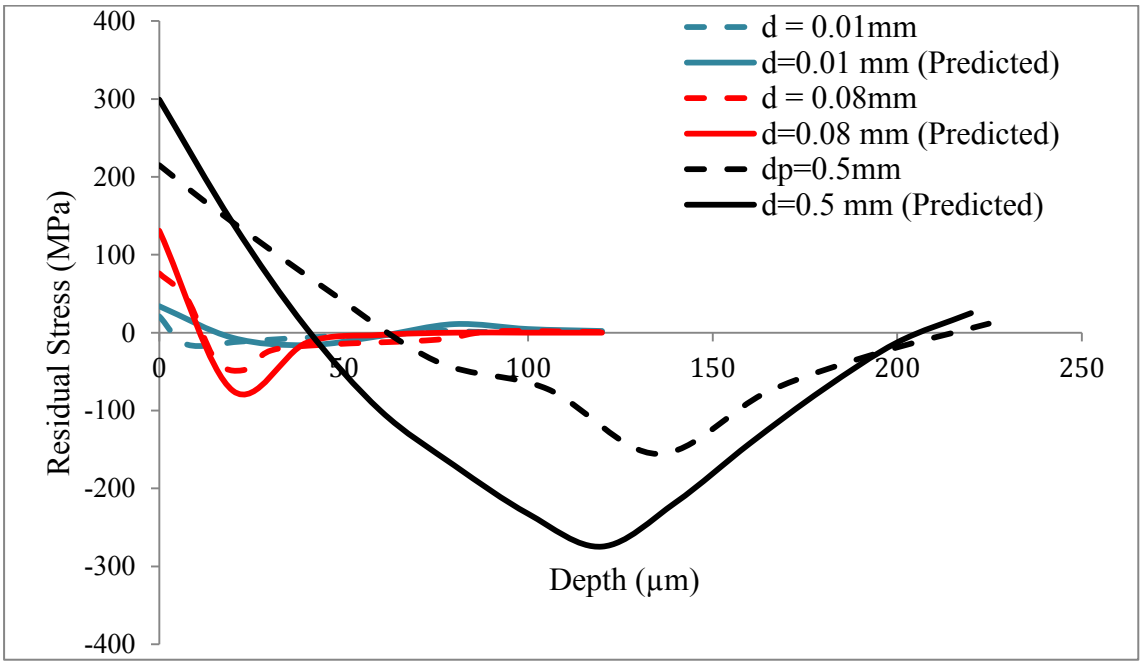

Figure 36: Predicted and experimental residual stress in Y direction.

Some comments can be made regarding the obtained experimental and theoretical work:

- The enhancement of the residual stress model helped to enhance the surface residual stress predictions. Before the enhancement, residual stresses were most of the time tensile.

- The regeneration was successfully implemented in the analytical modeling approach. The kinetic hardening helped to enhance the results.

- Simulated results were very close to the experimental work. Very light calibration procedure was performed through adapting the hybrid function that allows us to fine tune the model

- It is clear that the control of machining steps is important to ensure a compressive residual stress on the surface. This model can help in the optimization of machining processes.

- A last remaining assumption in the model has to be solved in the future regarding the elastic nature of the shear stresses. This assumption can still be a source of error in.

- The proposed novel analytical residual stress model to predict regeneration in multi-step machining included a kinematic hardening law to capture the cyclic plasticity, initial stress functions were used to capture the previous residual stresses in the new calculation. The agreement between simulations and experimental data prove the accuracy of the used method and it effect on the process mechanics.

5.6 CONCLUSION

Physics based understanding of residual stress regeneration in multi-steps machining operation is proposed using a combined elimination step and cyclic work hardening model. Initial stress functions are used to predict the new residual stress from the new machining pass. An enhanced residual stress model is also proposed in order to predict better residual stress results on the surface. The elastic assumption is replaced by a more realistic plastic assumption. The regeneration algorithm is implemented for the case of multi-step milling operation. The proposed model is able to capture the residual stress profile with a very high accuracy. The experimental and predicted results show that in the case of multi-step milling, the successive machining operation can be optimized in order to achieve a compressive surface stresses. The proposed model can therefore be utilized in designing machining operations to enhance surface integrity. The agreement between experiment and simulation supports the proposed utilization of the kinematic hardening associated with the initial stress functions..

REFERENCES

[1] Yamin Shao, Steven Liang Omar Fergani, "Effect of Temperature on the Subsurface Microstructure and Mechanical Properties of AA 7075-T6 in Machining," in Procedia CIRP, Nottingham, 2014.

[2] Yamin Shao, Ismail Lazoglu, Steven Liang Omar Fergani, "Temperature effect on grinding residual stresses," in Procedia CIRP, Berkley, 2014.

[3] Yamin Shao, Steven Y. Liang Omar Fergani, "Effect of Temperature on the Subsurface Microstructure and Mechanical Properties of AA 7075-T6 in Machining," Procedia CIRP, vol. 13, pp. 181-185, 2014.

[4] D. Umbrello, L. Settineri, I.S. Jawahir G. Rotella O.W. Dillon Jr., "Finite element modeling of microstructural changes in turning of AA7075-T651 Alloy," Journal of Manufacturing Processes, pp. 87-95, 2013.

[5] Yung C. Shin Hongtao Ding Ninggang Shen, "Modeling of grain refinement in aluminum and copper subjected to cutting," Computational Materials Science, pp. 3016–3025, 2011.

[6] M. Salahshoor, S.N. Melkote, T. Marusich R. Liu, "A unified internal state variable material model for inelastic deformation and microstructure evolution in SS304," Materials Science and Engineering: A, vol. 594, pp. 352-363, 2014.

[7] D. Rodriguez and J. A. Planell F. X. Gil, "grain growth kinetics of pure titanium," Scripta Mettalurgica et Meterialia, vol. 33, pp. 361-1366, 1995.

[8] Yamin Shao, Steven Y. Liang Omar Fergani, "Effect of Temperature on the Subsurface Microstructure and Mechanical Properties of AA 7075-T6 in Machining," Procedia CIRP, vol. 13, pp. 181-185, 2014.

[9] S. Basu, S. Shekhar, J. Cai, M.R. Shankar S. Abolghasem, "Mapping subgrain sizes resulting from severe simple shear deformation," Acta Materialia, vol. 60, pp. 376-386, 2012.

[10] Christopher Saldana, W. Dale Compton, Srinivasan Chandrasekar Yang Guo, "Controlling deformation and microstructure on machined surfaces," Acta materialia, vol. 59, pp. 4538-4547, 2011.

[11] ueda, Kazuaki iwata, Kazuo nakayama Kanji, "chip formation mechanism in single crystal cutting of β-brass," cirp annals - manufacturing technology, vol. 29, no. 1, pp. 41-46, 1980.

[12] Anish Roy, Tamer El Sayed, Vadim V. Silberschmidt Murat Demiral, "Numerical modelling of micro-machining of f.c.c. single crystal:Influence of strain gradients," 2014.

[13] Kota N, Ozdoganlar O Lawson Bl, "Effects of crystallographic anistropy on orthogonal micromachining of single-crystal aluminum," j. manuf. sci. eng, vol. 130, no. 3, pp. 031116-11, 2008.

[14] Anthony D. Rollett, O. Burak Ozdoganlar Nithyanand Kota, "A Rate-Sensitive

Plasticity-Based Model for Machining of Face-Centered Cubic Single-Crystals—Part I: Model Development," vol. 133, no. 3, 2011.

[15] K.h.w. seah, X.p. Li, M. Rahman M. Sharif Uddin, "Effect of crystallographic orientation on wear of diamond tools for nano-scale ductile cutting of silicon," Wear, vol. 257, no. 7-8, pp. 751-759, 2004.

[16] Yifan Dai, Ziwen Zheng, Hang Gao, Xiaoping Li Haofeng Chen, "Effect of crystallographic orientation on cutting forces and surface finish in ductile cutting of kdp crystals," machining science and technology, vol. 15, no. 2, 2011.

[17] S Abolghasem, S Basu, J Cai, M R Shankar S Shekhar, "Effect of Severe Plastic Deformation in Machining Elucidated via Rate-Strain-Microstructure (RSM) Mappings," ASME Journal of Manufacturing Science and Engineering, p. 031008, 2012.

[18] Yilong Wang, Guang Yu, Shen Dong, Xinzhou Zhang Qingliang Zhao, "Investigation of anisotropic mechanisms in ultra-precision diamond machining of KDP crystal," Journal of Materials Processing Technology, vol. 209, no. 8, pp. 4169-4177, 2009.

[19] Li X, Fergani O, Guo Yang j, Liang S Y. Venkatachalam S, "Crystallographic effects on microscale machining of polycrystalline brittle materials," j. micro nano-manuf, vol. 041001, no. 4, 2013.

[20] YC Ding. H Shin, "Dislocation density-based modeling of subsurface grain refinement with laser-induced shock compression," Computational Materials Science, vol. 53, no. 1, pp. 79-88, 2012.

[21] Steven Y Liang Omar Fergani, "Materials-affected manufacturing," vol. 1, no. 2-4, 2013.

[22] J Harza S Ramalingam, "Dynamic shear stress analysis of single crystal machining studies," vol. 95, no. 4, 1973.

[23] M.Eugene Merchant, "Mechanics of the metal cutting process. i. orthogonal cutting and a type 2 chip ," j. appl. phys., vol. 16, p. 267, 1945.

[24] I., Islam, C Lazoglu, "Modelling of 3d temperature fields for oblique machining," cirp annals, vol. 61/1, pp. 127-130, 2012.

[25] Robert Hill, "Theory of mechanical properties of fibre-strengthened materials—III. self-consistent model," Journal of the Mechanics and Physics of Solids, vol. 13, no. 4, pp. 189-198, 1965.

[26] C. N. TOME, P. PONTE CASTANEDA R. A. LEBENSOHN, "Self-consistent modelling of the mechanical behaviour," Acta Metallurgica et Materialia, vol. 87, no. 28, pp. 2611-2624.

[27] R. and C. Tomé Lebensohn, "A self-consistent anisotropic approach for the simulation of plastic deformation and texture development of polycrystals: application to zirconium alloys ," Acta Metallurgica et Materialia, vol. 41, no. 9, pp. 2611-2624, 1993.

[28] S lin, B adams, S ahzi Hamid Garmestani, "statistical continuum theory for texture evolution of polycrystals," journal of the mechanics and physics of solids, vol. 49, pp. 589-607, 2001.

[29] E Brinksmeier, R M'Saoubi, D K Aspinwall, J C Outeiro, D Meyer, D Umbrello, A D Jayal I S Jawahir, "Surface integrity in material removal processes: Recent advances," CIRP Annals - Manufacturing Technology, vol. 60, no. 2, pp. 603-626, 2011.

[30] D Ulutan, B E Alaca, S Engin I Lazoglu, "An enhanced analytical model for residual stress prediction in machining," CIRP Annals - Manufacturing Technology, vol. 57, no. 1, pp. 81-84, 2008.

[31] J C Su SY Liang, "Residual Stress Modeling in Orthogonal Machining," CIRP Annals - Manufacturing Technology, vol. 56, no. 1, pp. 65-68, 2007.

[32] Ismail Lazoglu, Ali Mkaddem, Mohamed El Mansori, Steven Y Liang Omar Fergani, "Analytical modeling of residual stress and the induced deflection of a milled thin plate," The International Journal of Advanced Manufacturing Technology, vol. 75, no. 1-4, pp. 455-463, 2014.

[33] F Salvatore, H Hamdi H Dehmani, "Numerical study of residual stress induced by multi-steps orthogonal cutting," in Procedia CIRP, 2013, pp. 299 – 304.

[34] T Obikawa, T Shirakashi H Sasahara, "FEM analysis on cutting sequence effect on mechanical characteristics on machined layer," Journal of Materials Processing Technology, vol. 62, no. 4, pp. 448-453, 1996.

[35] Balkrishna C. Rao, Srinivasan Chandrasekar M. Ravi Shankar, "Thermally stable nanostructured materials from severe plastic deformation of precipitation-treatable Ni-based alloys," Scripta Materialia , vol. 58, pp. 675–678, (2008).

[36] Christopher Saldana, W. Dale Compton, Srinivasan Chandrasekar Yang Guo, "Controlling deformation and microstructure on machined surfaces," Acta Materialia , vol. 59, pp. 4538–4547, (2011).

[37] A Characterization for the Flow Behavior of As-Extruded 7075 Aluminum, "Guo-zheng Quan, Gui-sheng Li, Yang Wang, Wen-quan Lv, Chun-tang Yu, Jie Zhou," Materials Research, vol. 16, no. 1, pp. 19-27, 2013.

[38] G. R., Cook, W. H. Johnson, "A constitutive model and data for metals subjected to large strains, strain rate and temperature," in 7th International Symposium on Ballistics, 1983, pp. 541-547.

[39] Karhausen K. Yanagimoto J, "Incremental formulation for the prediction of flow stress and microstructural change in hot forming," ournal of Manufacturing Science and Engineering , pp. 316–22, 1998.

[40] Wu-Chung Sue, Chi-Feng Lin, Chin-Jyi Wu Woei-Shyan Lee, "The strain rate and temperature dependence of the dynamic impact properties of 7075 aluminum alloy," Journal of Materials Processing Technology, vol. 100, pp. 116-122, 2000.

[41] Erik Nes, "Modelling of work hardening and stress saturation in FCC metals," Progress in Materials Science, vol. 41, no. 3, pp. 129-193, 1997.

[42] P. G. Shewmon, "The movement of small inclusions in solids by a temperature gradient," AIME TRANS, pp. 1134-1137, 1964.

[43] R.E. Reed-Hill, Physical Metallurgy Principles. New York: Van Nostrand , 1972.

[44] Srinivasan Chandrasekar , W. Dale Compton, Alexander H. King M. Ravi Shankar, "Characteristics of aluminum 6061-T6 deformed to large plastic strains by

machining," materials science and engineering, vol. 410-411, pp. 364-368, 2005.

[45] Tunnicliffe PJ, Patterson SJ. Sheppard T, "Direct and indirect extrusion of a high strength aerospace alloy (AA7075). ," Journal of Mechanics and Working Technology, pp. 313–31, 1982.

[46] Steven Y. Liang Kuan-Ming Li, "Modeling of cutting forces in near dry machining under tool wear effect," International Journal of Machine Tools and Manufacture, vol. 47, no. 7-8, pp. 1292-1301, 2007.

[47] Tabei A, Garmestani H, Liang SY Fergani O, "Prediction of polycrystalline materials texture evolution in machining via Viscoplastic," 2014.

[48] Xueping Zhang , C. Richard Liu Liqiang Ding, "Dislocation Density and Grain Size Evolution in the Machining of Al6061-T6 Alloys," J. Manuf. Sci. Eng, vol. 136, 2014.

[49] Masafumi Noda, Ryoichi Chiba, Mitsutoshi Kuroda Tsuyoshi Mayama, "Crystal plasticity analysis of texture development in magnesium alloy during extrusion," International Journal of Plasticity, vol. 27, no. 12, pp. 1916–1935, 2011.

[50] Ahmet Ekerim, Gizem Oktay Secgin, Ozgur Duygulu Selda Ucuncuoglu, "Effect of asymmetric rolling process on the microstructure, mechanical properties and texture of AZ31 magnesium alloys sheets produced by twin roll casting technique ," Journal of Magnesium and Alloys, vol. 2, no. 1, pp. 92–98, 2014.

[51] Wang H, "Evaluation of self-consistent polycrystal plasticity models for magnesium alloy AZ31B sheet," nternational Journal of Solids and Structures, vol. 47, no. 21, pp. 2905-2917., 2010.

[52] Wang H, "A crystal plasticity model for hexagonal close packed (HCP) crystals including twinning and de-twinning mechanisms," International Journal of Plasticity, vol. 49, no. 0, pp. 36-52., 2013.

[53] J.D Eshelby, "The determination of the elastic field of an ellipsoidal inclusion, and related problems.," Proceedings of the Royal Society of London. Series A. Mathematical and Physical Sciences, vol. 241, no. 1226, pp. 376-396, 1957.

[54] G.I Taylor, "Analysis of plastic strain in a cubic crystal.," Stephen Timoshenko 60th Anniversary , pp. 218-224, 1938.

[55] E Voce, "A practical strain-hardening function," Metallurgia, vol. 51, no. 307, pp. 219-226, 1955.

[56] M. Ravi Shankar , Seongyl Lee , Jihong Hwang, Srinivasan Chandrasekar , W. Dale Compton, Kevin P. Trumble Srinivasan Swaminathan, "Large strain deformation and ultra-fine grained materials by machining," Materials Science and Engineering A, vol. 410-411, pp. 358–363, 2005.

[57] P.L.B. Oxley, "An analysis for orthogonal cutting with restricted tool-chip contact," International Journal of Mechanical Sciences, vol. 4, no. 2, pp. 129-135, 1962.

[58] I. and Bugdayci, B Lazoglu, "Thermal Modeling of End Milling," CIRP Annals, vol. 63:1, pp. 113-116, 2014.

[59] Goodier Timoshenko, Theory of Elasticity. New York: Mcgraw-Hill, 1951.

[60] C Y Hui, A T Zehnder M T A Saif, "Interface shear stresses induced by non-uniform heating of a film on substrate.," Thin Solid Films, vol. 224, pp. 159-167, 1993.

[61] D L McDowell, "An approximate algorithm for elastic-plastic two-dimensional rolling/sliding contact," Wear, vol. 211, no. 2, pp. 237-246, 1997.

[62] Petch Hall, "The Cleavage Strength of Crystals," J. Iron & Steel Inst, vol. 174, pp. 25-28, 1950.

[63] C.Y Hui, A.T Zehnder M.T.A Saif, "Interface shear stresses induced by non-uniform heating of a film on a substrate," Thin Solid Films, pp. 159-167, 1993.